Exotically knotted surfaces

Alejandro García Rivas

Born 20th February 1998 in Barcelona, Spain

August 12, 2024

Master's Thesis Mathematics

Advisor: Dr. Isaac Sundberg

Second Advisor: Prof. Dr. Peter Teichner

Max Planck Institute for Mathematics

Mathematisch-Naturwissenschaftliche Fakultät der

Rheinischen Friedrich-Wilhelms-Universität Bonn

Contents

Introduction

In this work, we will study the following notion.

Definition. *Two smooth embeddings $S^n \hookrightarrow W^m$ are said to be exotically knotted if they are isotopic through ambient homeomorphisms, but not through diffeomorphisms.*

More specifically, we will focus on embeddings of surfaces in 4-manifolds. In this case, we are usually a bit sloppy with nomenclature and refer to the embedding $S^2 \hookrightarrow W^4$ as the surface S. In particular, we say that two surfaces S_1, S_2 are exotically knotted in W^4 when their embeddings are.

Some results concerning this are known for quite a while. First, there are some rigidity statements.

Theorem ([1])**.** *All biregular embeddings $\mathbb{C} \hookrightarrow \mathbb{C}^2$ are biregularly equivalent. In particular, there is no exotically knotted $\mathbb{C}$ birregularly embedded in $\mathbb{C}^2$.*

Theorem ([10])**.** *Let W^4 be a closed, simply-connected Kähler surface. Then, any two smooth, closed complex curves that are homologous[1] are also smoothly isotopic (through complex curves).*

Theorem ([17])**.** *There are no exotically knotted complex algebraic[2] curves in $\mathbb{C}^2$ with the topological type of a surface-with-1-hole.*

For a general topological type, this is an open problem. On the other hand, there are some known flexibility results.

Theorem (Freedman, 1985 and [13])**.** *There exist exotically knotted $\mathbb{R}^2$ and $\mathbb{R}^2 \smallsetminus \mathring{D}^2$ in $\mathbb{R}^4$.*

Theorem ([9])**.** *There exist exotically knotted closed non-orientable surfaces in S^4 and $\mathbb{R}^4$.*

Interestingly, the orientable case is still an open problem.

Theorem ([18])**.** *There is a pair of exotically knotted disks properly embedded in B^4.*

The rigidity exhibited by the algebraic setting and the flexibility shown in these last results might lead one to ask what happens when we reach a compromise between algebraic and smooth embeddings. Kyle Hayden recently answered this question when the compromise is *holomorphic embedding.*

Theorem A ([17])**.** *There are infinitely many pairs of proper holomorphic curves in $\mathbb{C}^2$ that are exotically knotted.*

One of the main goals of this work is to present Hayden's construction in detail. Along this path, we will also present some remarkable results. In particular:

Theorem B ([17])**.** *There is a pair of exotically knotted disks properly embedded in B^4 relative boundary.* [3]

We will present a proof of this using corks (cf. Definition 2.0.1). However, later on we will use a different method to prove a generalization of this result (see Theorem E below).

Theorem C ([17])**.** *Any compact, connected, orientable surface with boundary (other than the disk) admits a pair of smooth, proper embeddings in B^4 that are exotically knotted. Furthermore, they remain exotically knotted when restricted to the interior.*

[1] This is automatic if they are topologically isotopic

[2] i.e. given as the zero-locus of a complex polynomial

[3] The term *relative boundary* simply means that the ambient topological isotopy fixes S^3 pointwise and that there is no ambient smooth isotopy fixing S^3 pointwise. Hence, this result is weaker than Hayden's result above.

The idea behind the proof of these two results is similar in essence. First, the surfaces are proven to be topologically isotopic using a recent result from Conway and Powell (cf. Theorem 3.1.3). Then, the smooth isotopy is obstructed by distinguishing facets of the double branched covers along them.

The next step towards Theorem A is to realize these surfaces as compact pieces of complex algebraic curves. This will be done simply by realizing them as positively braided surfaces and then use Rudolph's work ([23]), which guarantees that such surfaces are smoothly isotopic to compact pieces of complex algebraic curves.

Finally, Hayden's construction of exotically knotted complex holomorphic curves will be completed by locating a suitable Fatou-Bieberbach domain $\Omega \subset \mathbb{C}^2$ and use it to reembed these algebraic surfaces holomorphically into $\mathbb{C}^2$.

On the other hand, using these same techniques, we extend the construction in several directions. First, we generalize Theorem B by constructing arbitrarily large tuples of pairwise exotically knotted surfaces in B^4 relative boundary. We do this for any compact, connected surface, even the non-orientable ones. More precisely, we show:

Theorem D. *Let $n \in \mathbb{N}$. Any compact, connected surface with boundary admits a 2^n-tuple of smooth, proper embeddings in B^4 that are pairwise exotically knotted relative boundary.*

Next, we generalize Theorem C to non-orientable surfaces. Namely, we show:

Theorem E. *Any compact, connected, non-orientable surface with boundary admits a pair of smooth, proper embeddings in B^4 that are exotically knotted. Furthermore, they remain exotically knotted when restricted to the interior.*

Finally, we will also be able to extend Theorem C to larger tuples of exotically knotted embeddings. This construction, though, does not work in the non-orientable case. We prove:

Theorem F. *Let $g \geq 0, h \geq 1 \in \mathbb{N}$ not both equalities. The compact, connected, orientable surface with boundary with-h-holes and genus g admits a $(g+1)h$-tuple of smooth, proper embeddings in B^4 that are pairwise exotically knotted. Furthermore, they remain exotically knotted when restricted to the interior.*

This work is organized as follows. In Chapter 1, we introduce the basic definitions and results regarding handlebodies and Kirby calculus.

In Chapter 2, we switch topic to introduce contact structures and Legendrian knots. The goal of this is to give sufficient and necessary conditions for a 4-manifold to admit a Stein structure, as the Stein setting will allow us later on to obstruct surfaces from being smoothly isotopic. We also define corks and use the rigidity of Stein structures to prove that the positron cork (cf. Figure 2.1) is indeed a cork.

In Chapter 3, we describe Hayden's construction. Namely, we show Theorems A, B and C.

Finally, in Chapter 4, we extend the construction and prove the remaining theorems D, E and F.

Acknowledgments

First of all, I would like to thank Isaac for the supervision and, mostly, for time they have dedicated to me. Truly, all the meetings and conversations have been meaningful for this work and for my academic life.

Secondly, I wanted to thank Pete and Aru for the weekly talks and the nice and healthy environment they granted. I have learned a lot from them and I have always felt very comfortable.

I would also like to thank my parents for supporting me to study this master abroad and for many other uncountable reasons.

Finally, I want to thank my friends in Bonn, especially Jose, for being there, for taking good care of each other and, of course, for making me happy.

Chapter 1

Preliminary topics

In this chapter, we present the fundamental tools for the development of the next chapters. We start in Section 1.1 by giving basic results concerning *handle decompositions* in general dimension.

In Section 1.2, we specialize the theory of the previous section to the 4-dimensional case. We introduce *Kirby diagrams*, explain how to manipulate them and how to extract information from them.

In Section 1.3, we describe how to compute Kirby diagrams of branched covers.

1.1 Handle decompositions

In this section, we define handle decompositions and state some fundamental results about them.

Definition 1.1.1. Let $0 \leq k \leq n$. An *n-dimensional k-handle* is the manifold with corners $h^{k,n} = D^k \times D^{n-k}$. The integer k is called the *index* of the handle. Furthermore, the following subsets of $h^{k,n}$ are defined:

- Core: $D^k \times 0$
- Attaching sphere: $S^{k-1} \times 0$
- Attaching region: $S^{k-1} \times D^{n-k}$
- Cocore: $0 \times D^{n-k}$
- Belt sphere: $0 \times S^{n-k-1}$
- Belt tube: $D^k \times S^{n-k-1}$

The following figures depict a 2-dimensional 1-handle and its anatomy.

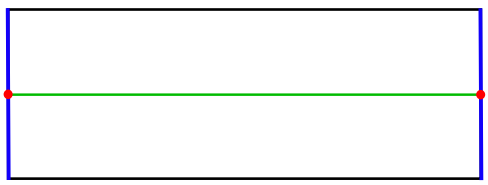

Figure 1.1: Core, attaching sphere and attaching region.

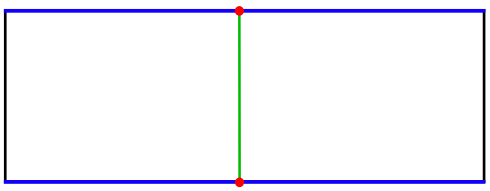

Figure 1.2: Cocore, belt sphere and belt tube.

Definition 1.1.2. Let M be an n-manifold with boundary. Attaching a k-handle to M along an embedding $\varphi : S^{k-1} \times D^{n-k} \hookrightarrow \partial M$ consists of gluing a k-handle $h^{k,n}$ to M along φ to obtain the resulting manifold $M \cup_\varphi h^{k,n}$. After canonically smoothing the corners, we may assume that this new manifold is smooth.

In fact, since we will only care about the diffeomorphism type of the manifolds, by the Isotopy Extension Theorem, the embedding φ will only matter up to isotopy. By the Tubular Neighborhood Theorem ([15]), we may specify the (isotopy class of the) embedding $\varphi : S^{k-1} \times D^{n-k} \hookrightarrow \partial M$ above by the following two pieces of data:

(1) an embedding $\varphi_0 : S^{k-1} \hookrightarrow \partial M$ with trivial normal bundle, and

(2) a framing f of its normal bundle, i.e. an identification of $\nu\varphi_0(S^{k-1}) \subset \partial M$ with $S^{k-1} \times \mathbb{R}^{n-k}$.

Notice that two trivializations of the bundle $S^{k-1} \times \mathbb{R}^{n-k} \to S^{k-1}$ are related by a map $S^{k-1} \to GL(n-k)$. It follows that two isotopy classes of trivializations are related by an element of $\pi_{k-1}(GL(n-k)) \cong \pi_{k-1}(O(n-k))$. Hence, the second piece of data above is determined (non-canonically) by an element of $\pi_{k-1}(O(n-k), id)$.

The groups $\pi_i(O(m))$ are not known for all values of i and m, but the low-dimensional cases have been computed. We will particularly care about the column $n = 4$ of Table 1.1. It is worth mentioning that the fact that $\pi_0(O(n-1)) \cong \mathbb{Z}_2$ will not matter to us, as we will only consider orientable manifolds. In particular, there will be a unique way to attach 1-handles (provided $\partial_+ M$ is connected).

$k \diagdown n$	1	2	3	4
1	-	$\mathbb{Z}_2$	$\mathbb{Z}_2$	$\mathbb{Z}_2$
2	-	-	$\mathbb{Z}_2$	$\mathbb{Z}$
3	-	-	-	0
4	-	-	-	-

Table 1.1: Values of $\pi_{k-1}(O(n-k))$.

It is the fundamental result of Morse Theory, that any smooth compact manifold can be described by handle attachments. We now formalize this statement. Let M be a compact smooth n-manifold with boundary $\partial M = \partial_+ M \sqcup \partial_- M$. If M is oriented, choose orientations for $\partial_\pm M$ so that $\partial M = \partial_+ M \sqcup \overline{\partial_- M}$ with the induced boundary orientation.

Definition 1.1.3. A *handle decomposition* of M (relative to $\partial_- M$) is a diffeomorphism $\phi : M \to X$, where X is a manifold obtained from $I \times \partial_- M$ by attaching handles to its upper boundary and $\phi(\partial_- M) = \{0\} \times \partial_- M$.

Definition 1.1.4. A smooth function $f : M \to [0,1]$ is *Morse* if

- $f^{-1}(0) = \partial_- M$, $f^{-1}(1) = \partial_+ M$, and
- every critical point is non-degenerate.

For a non-degenerate critical point x of f, define its *index* as the number of negative eigenvalues of the Hessian of f at x and denote it by $\mathrm{ind}(x)$.

Lemma 1.1.5 ([22], §3)**.** *Let $f : M \to [0,1]$ be a Morse function. Then:*

(i) If f has no critical points, then $M \cong \partial_- M \times I$.

(ii) If f has exactly one critical point of index k, then $M \cong (\partial_- M \times [0,1]) \cup_\varphi h^{k,n}$ attached to the upper boundary.

Lemma 1.1.6 ([22], Corollary 6.7)**.** *Morse functions are dense in the set of smooth functions.*

Corollary 1.1.7. *M admits a handle decomposition relative to $\partial_- M$.*

Proof. By the previous lemma, there exists a Morse function $f : M \to [0,1]$. Since M is compact and non-degenerate critical points are isolated, f has a finite number of them. Repeated application of Lemma 1.1.5 yields a handle decomposition of M. □

Having discussed the existence of handle decompositions, our next goal is to give rules to simplify them, i.e. to sort the handles by increasing index, to cancel them whenever there is redundancy, etc. We record these fundamental rules.

Proposition 1.1.8 ([21], Theorem 4.8)**.** *The handle decomposition can be chosen so that the handles are attached in order of increasing index. Handles of the same index can be attached in any order (or simultaneously).*

From now on, we will implicitly be considering only handle decompositions satisfying the above property.

Proposition 1.1.9 ([21], Theorem 5.4)**.** *If the attaching sphere of a k-handle intersects the belt sphere of a $(k-1)$-handle transversely in a single point, then these handles can be cancelled.*

Later on, we will see examples on how to use this in dimension 4.

To end this section, we discuss how to compute π_1 and H_* from a handle decomposition. Since k-handle attachments are just thickened k-cell attachments, a handle decomposition yields a CW decomposition. In particular, the fundamental group and the homology are computed as in the case of CW complexes.

Theorem 1.1.10 ([14], computation of π_1)**.** *Suppose M is orientable, has $\partial_- M = \varnothing$ and has a handle decomposition with a unique 0-handle. Let M_1 be the 1-skeleton of the handle decomposition, i.e. $M_1 = 0$-handle $\cup$ m 1-handles. Fix a point $*$ in the 0-handle. Let a_i be the loop based at $*$ going around the i-th 1-handle once. Then, $\pi_1(M_1, *)$ is freely generated by the loops $a_1, \dots, a_m$. Furthermore, a presentation of $\pi_1(M, *)$ is given by*

$$\pi_1 M \cong \langle a_1, \dots, a_m | r_1, \dots, r_l \rangle,$$

where $r_j \in \pi_1 M_1$ is the homotopy class of the attaching sphere of the $j-$th 2-handle (i.e. a word in $a_1, \dots, a_m$).

Now we describe how to compute the homology $H_*(-;\mathbb{Z})$ of an arbitrary compact orientable manifold pair $(M, \partial_- M)$ given a handle decomposition of M relative to $\partial_- M$. Denote by M_k the k-skeleton of M. Set $M_{-1} = \partial_- M$. Define $C_k = H_k(M_k, M_{k-1}; \mathbb{Z})$ and $\partial_k : C_k \to C_{k-1}$ as the connecting homomorphism in the long exact sequence in homology of the triple (M_k, M_{k-1}, M_{k-2}).

Lemma 1.1.11 ([21], 3.15 and 7.4)**.** *The following properties are satisfied:*

(i) $H_i(M_k, M_{k-1}; \mathbb{Z}) \cong \begin{cases} \mathbb{Z}[\{k - \text{handles}\}], & i = k \\ 0, & \text{else} \end{cases}$. *In particular,* $C_k \cong \mathbb{Z}[\{k - \text{handles}\}]$.

(ii) (C_*, ∂_*) is a chain complex and $H_k(M, \partial_- M; \mathbb{Z}) \cong H_k(C_*)$ for every k.

Hence, in order to compute the homology of the pair $(M, \partial_- M)$, it will suffice to understand the differential $\partial_k : C_k \to C_{k-1}$.

Theorem 1.1.12 ([21], 7.3)**.** *(Computation of H_*) Let $\{h_i^k\}$ be the collection of k-handles in a handle decomposition of M relative to $\partial_- M$. Fix an orientation of M and an orientation on the core and the cocore of each handle that makes the three of them compatible. Let λ_{ij} be the intersection number of the attaching sphere of h_i^k and the belt sphere of h_j^{k-1} in $\partial_+ M_k$ with the induced orientations. Then, the matrix of $\partial_k : C_k \to C_{k-1}$ with respect to the bases $\{h_i^k\}$ of C_k is (λ_{ij}).*

1.2 Kirby calculus

The goal of this section is to define Kirby diagrams and state rules for both manipulating them and for extracting data such as their fundamental group, homology and intersection form. From now on, unless otherwise stated, all manifolds will be assumed to be orientable and of dimension 4.

We begin with a simple, yet very useful observation. With the notation of the previous section, suppose we attach a 1-handle to a manifold M. By Proposition 1.1.9, we can further attach a cancelling 2-handle to obtain a diffeomorphism

$$M \cup \text{1-handle} \cup \text{2-handle} \cong M.$$

Thus, attaching a 1-handle is the same as removing a cancelling 2-handle. Notice that the cocore of such a 2-handle is an unknotted disk in ∂M whose interior is pushed into the interior of M. Hence, attaching a 1-handle to M is equivalent to removing a tubular neighborhood of such a disk. This gives a very convenient way to think about 1-handles. In fact, we define:

Definition 1.2.1. A *Kirby diagram* is a link $L = (U_1, \dots, U_m, K_1, \dots, K_l)$ in S^3 such that

(1) $U_1 \cup \dots, U_m$ is an unlink, and

(2) each K_j is a framed knot, i.e. comes together with an integer f_j called *framing coefficient* of K_j.

Kirby diagrams are supposed to represent a 4-dimensional handle decomposition with a single 0-handle, m 1-handles and l 2-handles. We interpret them as follows. First, the ambient space S^3 represents the boundary ∂D^4 of the 0-handle.

Secondly, each U_i represents a 1-handle attachment in the sense of the observation above. Indeed, it is a standard fact that any collection of smoothly embedded disjoint disks in S^3 is unique up to isotopy relative boundary. Hence, there is no ambiguity if we avoid drawing the disks whose interior is pushed into the interior of D^4, so we just need to consider the boundaries $U_1, \dots, U_m$ of these disks.

Lastly, each K_j represents the attaching sphere of a 2-handle. Recall from Table 1.1 and the discussion above it, that a 2-handle attachment also requires the additional data of a framing of the normal bundle of K_j in $\partial(D^4 \cup \text{1-handles}) = \#_m S^1 \times S^2$. Since $\pi_1(O(2)) \cong \mathbb{Z}$ (cf. Table 1.1), the framing is determined by an integer in a (a priori) non-canonical way. More precisely, we must choose a base framing F_0 so that any other framing F is determined by an integer k relating them. However, since K_j is a knot in S^3, there is already a canonical framing for K_j, obtained by the outer normal field of a Seifert surface for K_j. We may thus take this canonical framing to be F_0 and describe any other framing by the framing coefficient f_j.

When drawing Kirby diagrams, we will picture the unknots U_i as black dotted circles. On the other hand, the knots K_j will have their framing coefficient next to them. The following are the simplest examples of Kirby diagrams:

Figure 1.3: Kirby diagrams for $S^1 \times D^3$ (left) and $S^2 \times D^2$ (right).

We now describe the rules we will be using in this work to manipulate Kirby diagrams. We say that two Kirby diagrams are *equivalent* if they represent diffeomorphic manifolds. We first describe handle slides.

Proposition 1.2.2 ([14], §5.1)**.** *Let $L = (U_1, \dots, U_m, K_1, \dots, K_l)$ be a Kirby diagram. Fix a pair of 2-handles h_i, h_j attached along K_i and K_j, respectively. The following procedure, called* sliding h_i over h_j*, yields an equivalent Kirby diagram L':*

(1) Fix orientations on K_i and K_j.

(2) Let $\bar{K}_j$ be a (close enough) parallel copy of K_j determining the framing f_j.

(3) Let K_i' be the connected sum of K_i and $\bar{K}_j$ along some band.

(4) Let L' be the Kirby diagram L with K_i replaced by K_i' and the framing coefficient f_i replaced by $f_i' = f_i + f_j \pm 2lk(K_i, K_j)$, where the $+$ sign is taken if the connected sum respected the fixed orientations of K_i and K_j. Otherwise, the $-$ sign is taken.

Proposition 1.2.3 ([14], §5.4)**.** *Let $L = (U_1, \dots, U_m, K_1, \dots, K_l)$ be a Kirby diagram. Fix a pair of 1-handles h_i, h_j represented by dotted circles U_i, U_j, respectively. The following procedure, called* sliding h_j over h_i*, yields an equivalent Kirby diagram L':*

(1) Let $\bar{U}_j$ be a (close enough) parallel copy of U_j determining the 0-framing.

(2) Fix a plane separating U_i and $\bar{U}_j$ and disjoint from any other dotted circles.

(3) Let U_i' be the connected sum of U_i and $\bar{U}_j$ along some band whose core intersects the plane once.

(4) Let L' be the Kirby diagram L with U_i replaced by U_i'.

Notice that sliding a 1-handle over another is (up to some details) the same procedure as sliding a 0-framed 2-handle over another. One can also slide a 2-handle over a 1-handle (cf. [14] §5.4), but we will not use it in this work.

We now describe how handle cancellation affects Kirby diagrams.

Proposition 1.2.4 ([14], §5.4)**.** *Let $L = (U_1, \dots, U_m, K_1, \dots, K_l)$ be a Kirby diagram. Suppose that K_j intersects the Seifert disk of U_i in a unique point and no other $K_{j'}$ intersects the disk. Then, the Kirby diagram obtained from L by removing U_i and K_j is equivalent to L.*

If some other $K_{j'}$ intersects the disk, we can use Proposition 1.2.2 to slide it away so that it does not intersect the disk anymore. Doing this for every such $K_{j'}$, the intersection condition of the above Proposition can always be arranged.

In the content of this work, there are plenty of examples of these rules being used.

We now move on to explain how to compute π_1, H_* and the intersection form from a Kirby diagram. This will mostly follow immediately from Theorems 1.1.10 and 1.1.12.

Proposition 1.2.5. *Let $L = (U_1, \dots, U_m, K_1, \dots, K_l)$ be a Kirby diagram and M be the 4-manifold it represents. Let D_i be the Seifert disk of U_i and fix an orientation on all of them. Fix also an orientation of each K_j. A presentation of $\pi_1 M$ is given by*

$$\pi_1 M \cong \langle D_1, \dots, D_m | r_1, \dots, r_l \rangle,$$

where r_j is the word in $D_1, \dots, D_m$ obtained by tracking K_j along its orientation and writing D_i every time K_j intersects D_i matching the chosen orientation and writing D_i^{-1} otherwise.

Remark 1.2.6. For explicit generators of $\pi_1 M$, just consider the loops a_i that go around U_i once, matching the orientation of D_i, and do not intersect any other Seifert disk.

Proposition 1.2.7. *Let $L = (U_1, \dots, U_m, K_1, \dots, K_l)$ be a Kirby diagram and M be the 4-manifold it represents. Let D_i be the Seifert disk of U_i and fix an orientation on all of them. Fix also an orientation of each K_j. Let λ_{ij} be the (algebraic) intersection number of D_i and K_j. The homology $H_*(M;\mathbb{Z})$ is isomorphic to the homology of the chain complex*

$$0 \longrightarrow \mathbb{Z}^l \xrightarrow{\varphi} \mathbb{Z}^m \xrightarrow{0} \mathbb{Z} \longrightarrow 0,$$

where $\varphi : \mathbb{Z}^l \to \mathbb{Z}^m$ has matrix (λ_{ij}).

Remark 1.2.8. Again, for explicit generators of $H_1(M;\mathbb{Z})$ we may take the loops a_i of the remark above. We can also visualize explicit generators of $H_2(M,\mathbb{Z})$ under certain circumstances. Suppose K_j does not intersect any disk D_i. By the proposition, K_j must represent a generator of a $\mathbb{Z}$ summand of $H_2(M;\mathbb{Z})$. We may realize this generator as follows. K_j admits a Seifert surface F_j disjoint from the disks D_i. Orient it with the chosen orientation of K_j. Push the interior of F_j into the interior of D^4 and cap it off with the core of the 2-handle to obtain a closed surface $\hat{F}_j$. Orient $\hat{F}_j$ with the orientation of F_j. Then, $\hat{F}_j$ represents the aforementioned generator of the $\mathbb{Z}$ summand of $H_2(M;\mathbb{Z})$.

Finally, we deal with the intersection form.

Definition 1.2.9. Let $L = (U_1, \dots, U_m, K_1, \dots, K_l)$ be a Kirby diagram. Pick an orientation for every K_i. The *linking matrix* (Q_{ij}) of L is the $l \times l$ matrix given by

$$Q_{ij} = \begin{cases} f_i & i = j \\ lk(K_i, K_j), & i \neq j \end{cases}$$

Proposition 1.2.10. *Let $L = (K_1, \dots, K_l)$ be a Kirby diagram with no dotted circles and M be the 4-manifold it represents. Pick an orientation for every K_i. With respect to the basis $\{[\hat{F}_j]\}$ of $H_2(M;\mathbb{Z})$ described in Remark 1.2.8, the matrix of the intersection form $Q_M : H_2(M;\mathbb{Z}) \times H_2(M;\mathbb{Z}) \to \mathbb{Z}$ is the linking matrix (Q_{ij}).*

Remark 1.2.11. If L contains dotted circles, the corresponding result is true for the knots K_j that do not intersect any disk D_i, i.e. $[\hat{F}_j] \cdot [\hat{F}_{j'}] = Q_M([\hat{F}_j], [\hat{F}_{j'}]) = Q_{jj'}$.

1.3 Double branched covers

The goal of this section is to build up a method to compute Kirby diagrams of double branched covers. We first define branched covers, present some low-dimensional visual examples and then move on to explain a general method in dimension 4.

Definition 1.3.1. A *d-fold cyclic branched covering* $f : X^n \to Y^n$ with *branch locus* B^{n-2} embedded in Y^n is a smooth proper map such that

(1) $f_{|X \setminus f^{-1}(B)} : X \setminus f^{-1}(B) \to Y \setminus B$ is a d-fold cyclic cover, and

(2) $\forall p \in f^{-1}(B)$, there are coordinates around p so that f is

$$\begin{aligned} \mathbb{C} \times \mathbb{R}^{n-2}_+ &\to \mathbb{C} \times \mathbb{R}^{n-2}_+ \\ (z, x) &\mapsto (z^m, x). \end{aligned}$$

The integer m is called the *branching index* of f at p.

More importantly for our purposes, if $d = 2$, $f : X \to Y$ will be called *double branched covering* and the space X will be called *double branched cover* of Y along B.

Example 1.3.2. D^2 covers D^2 branched along one point.

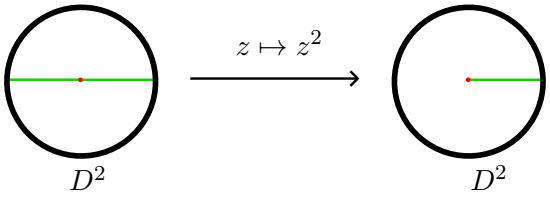

Figure 1.4: D^2 branched along the origin.

Example 1.3.3. Similarly, S^2 covers S^2 branched along two points.

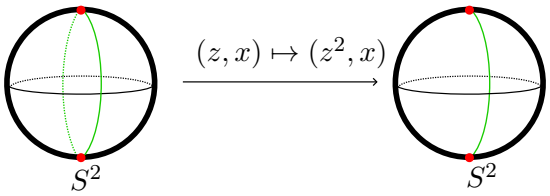

Figure 1.5: S^2 branched along the poles.

The following proposition, and especially its proof, give a recipe to construct X^n given (Y^n, B^{n-2}).

Proposition 1.3.4. *Given (Y^n, B^{n-2}), a surjective homomorphism $\pi_1(Y \setminus B) \twoheadrightarrow \mathbb{Z}_d$ determines a unique d-fold cyclic branched cover X of Y along B up to diffeomorphism.*

Proof. A surjective homomorphism $\pi_1(Y \setminus B) \twoheadrightarrow \mathbb{Z}_d$ determines an index-d subgroup of $\pi_1(Y \setminus \nu B)$. By standard covering space theory, this determines a unique d-fold cyclic cover of $Y \setminus \nu B$. Notice that an m-fold branched action along F is seen on νF as a map

$$\begin{aligned} \nu F \cong D^2 \times F &\to D^2 \times F \cong \nu F \\ (z, x) &\mapsto (z^m, x), \end{aligned}$$

The d-fold cyclic branched cover is then obtained by gluing νF back in using the map

$$\begin{aligned} S^1 \times F &\to S^1 \times F \\ (z, x) &\mapsto (z^m, x), \end{aligned}$$

so that condition (2) of Definition 1.3.1 is satisfied. Also, condition (2) determines the gluing map, so the d-fold cyclic branched cover is unique up to diffeomorphism. □

Example 1.3.5. Let us construct double branched covers of D^2 along two points. Notice that $\pi_1(D^2 \setminus \{x, y\}) \cong \mathbb{Z} * \mathbb{Z}$, and there are different surjections $\mathbb{Z} * \mathbb{Z} \to \mathbb{Z}_2$, each of which will yield a different cover. Let's say we pick the surjection $\gamma_x, \gamma_y \mapsto 1$. Following the procedure in the proof of Proposition 1.3.4, we first remove a tubular neighborhood of the points x, y in D^2. Then, we construct the double cover of $D^2 \setminus \nu x \cup \nu y$ associated to the chosen surjection. This is the top map in Figure 1.7. Finally, we fill the tubular neighborhoods back in to obtain the bottom map. In particular, this double branched cover of D^2 along two points is an annulus.

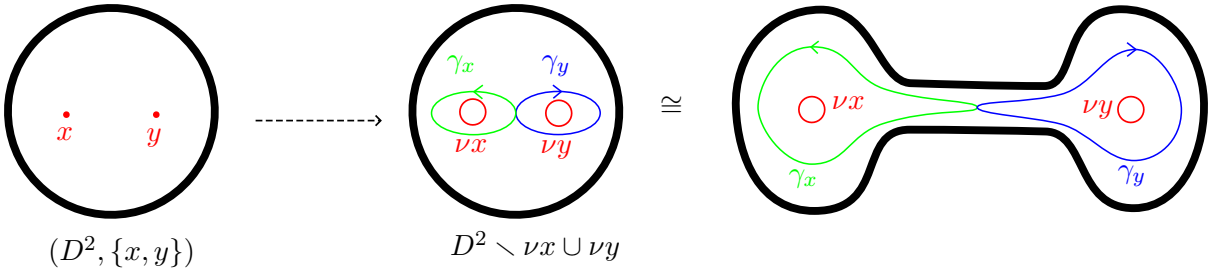

Figure 1.6: The complement $D^2 \smallsetminus \{\nu x, \nu y\}$.

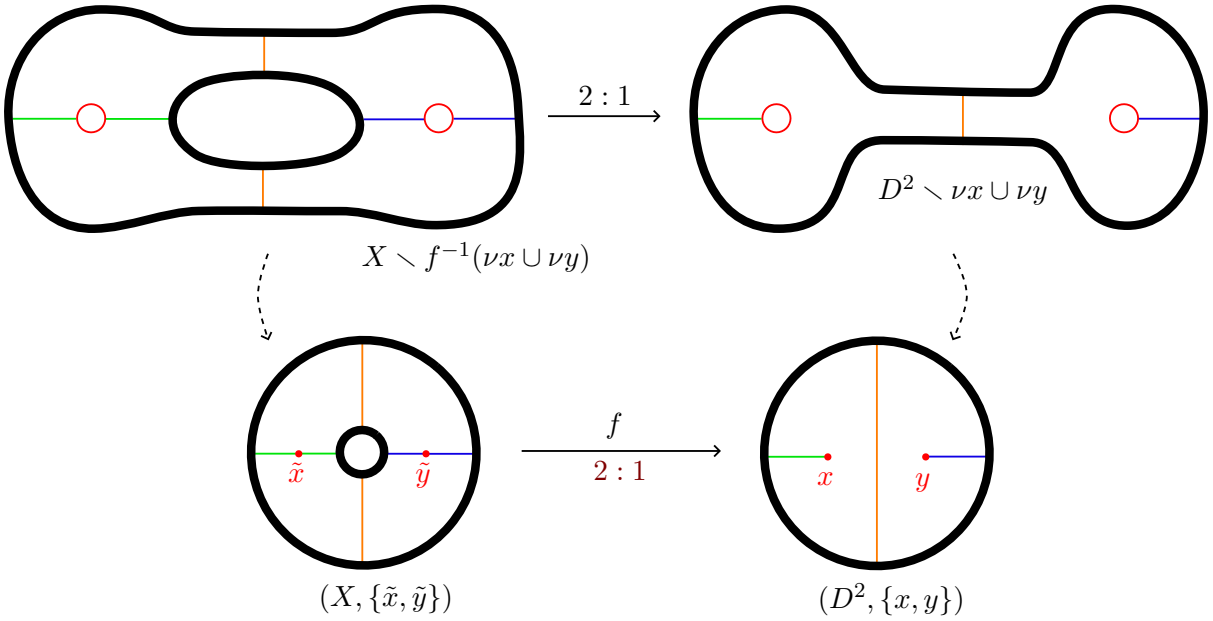

Figure 1.7: The double cover $X \smallsetminus f^{-1}(\nu x \cup \nu y) \to D^2 \smallsetminus \nu x \cup \nu y$ (above) and the double branched cover $f : X \to D^2$ (below).

This example is a good representative of the procedure used to construct branched covers in larger dimensions. Our goal now is to describe the general method we will use to construct double branched covers of B^4 along compact, connected, orientable, properly embedded surfaces $(F^2, \partial F^2)$ in (B^4, S^3). We begin by noticing:

Proposition 1.3.6. *There is a unique surjective map $\pi_1(B^4 \smallsetminus F^2) \twoheadrightarrow \mathbb{Z}_2$. In particular, we may unambiguously talk about* the *double branched cover of B^4 along F^2, which we denote by $\Sigma_2(B^4, F^2)$.*

Proof. It suffices to check that $H_1(B^4 \smallsetminus F^2) \cong \mathbb{Z}$ (integer coefficients are to be assumed unless otherwise stated), as this is the abelianization of $\pi_1(B^4 \smallsetminus F^2)$ and there is a unique surjective homomorphism $\mathbb{Z} \twoheadrightarrow \mathbb{Z}_2$. Consider the Mayer-Vietoris sequence associated to the decomposition $B^4 = (B^4 \smallsetminus F^2) \cup \nu F^2$:

$$\begin{array}{ccccccccc} H_2(B^4) & \longrightarrow & H_1(\nu F \smallsetminus F) & \longrightarrow & H_1(B^4 \smallsetminus F) \oplus H_1(\nu F) & \longrightarrow & H_1(B^4) \\ \| & & \wr\| & & \wr\| & & \| \\ 0 & \longrightarrow & H_1(S^1) \oplus H_1(F) & \longrightarrow & H_1(B^4 \smallsetminus F) \oplus H_1(F) & \longrightarrow & 0 \end{array}$$

Since the $H_1(F)$ summand on the left gets mapped to the $H_1(F)$ summand on the right under the identifications we made, we have an isomorphism $H_1(B^4 \smallsetminus F^2) \cong H_1(S^1) \cong \mathbb{Z}$. □

Remark 1.3.7. If F^2 is non-orientable, then the same argument shows that $H_1(B^4 \smallsetminus F^2) \cong \mathbb{Z}_2$, and so in this case, there is also a unique double branched cover.

As the proof of Proposition 1.3.4 and the previous examples suggest, our general method will begin by constructing the double cover of $B^4 \smallsetminus \nu F^2$. Computing Kirby diagrams of such complements is fairly standard and the general procedure can be found in [14], §6.2. Once we have a Kirby diagram of the complement $B^4 \smallsetminus \nu F^2$, we can obtain a Kirby diagram of its double cover using the following:

Lemma 1.3.8. *Suppose Y^4 is the 4-manifold with boundary given by the Kirby diagram*

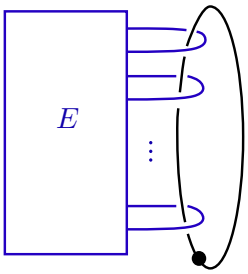

Figure 1.8: Kirby diagram for Y^4.

where the tangle E is allowed to contain several 1-handles and 2-handles. Let X^4 be the double cover of Y^4 associated to the surjective homomorphism $\pi_1(Y) \twoheadrightarrow \mathbb{Z}_2$ that sends the black 1-handle to 1 and the rest of the 1-handles (if any) to 0. Then, X^4 is given by the Kirby diagram

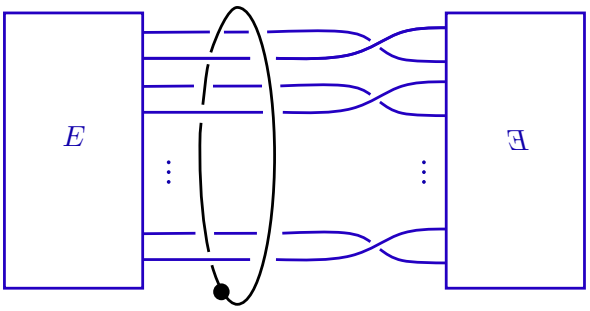

Figure 1.9: Kirby diagram for X^4.

The framing coefficient $fr(h_X)$ of a 2-handle h_X in the latter diagram can be computed via the formula:

$$fr(h_X) = fr(h_Y) + wr(h_X) - wr(h_Y) - k/2, \tag{1.1}$$

where h_Y is the 2-handle in Y^4 to which it projects and k is the number of times h_Y goes around the black dotted circle.[1]

Proof. Consider the "thickened diagram", which is equivalent to the Kirby diagram in Figure 1.8:

[1]Notice that this must be an even number, otherwise there would be no surjective map $\pi_1(Y) \twoheadrightarrow \mathbb{Z}_2$.

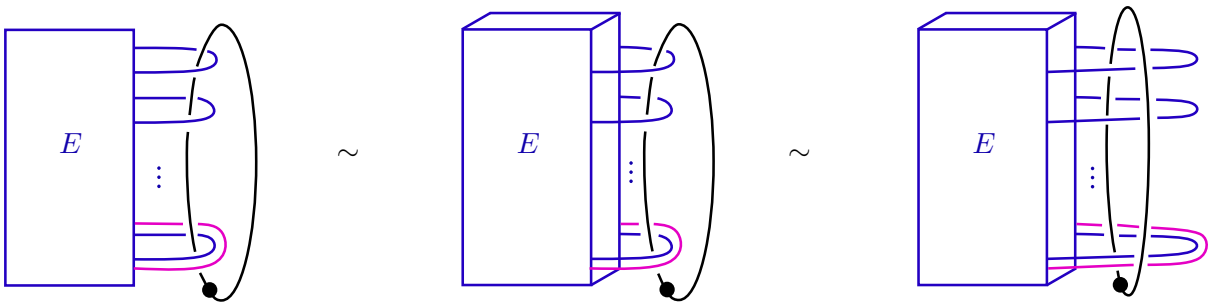

Figure 1.10: Equivalent Kirby diagrams for Y^4. The pink line is a piece of a push-off representing the blackboard framing.

In the rightmost diagram, we can take the wanted double cover by picturing the action $z \mapsto z^2$ around the black dotted circle:

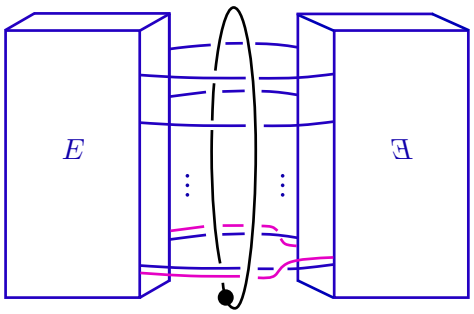

Figure 1.11: Thickened Kirby diagram for X^4. The pink lines are the lifts of the pink line of Figure 1.10.

Finally, by flattening this last diagram, we obtain:

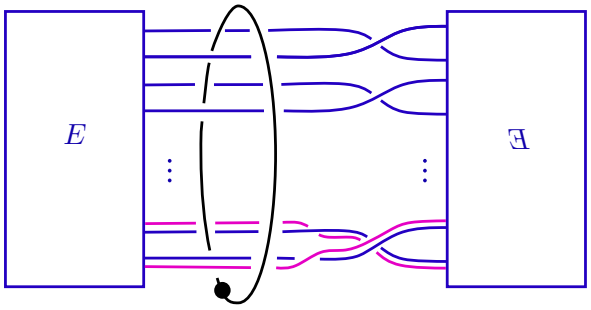

Figure 1.12: Kirby diagram for X^4. The pink lines are the lifts of the pink line of Figure 1.10.

By following the pink lines throughout this process, we get that the blackboard framing lifts to the blackboard framing plus a negative half-twist every time the 2-handle goes around the black dotted circle. Hence, we obtain Equation 1.1. □

According to Proposition 1.3.4, we now need to fill lifts of νF into the double cover of $B^4 \setminus \nu F$. Fortunately, we will be only interested in the double branched cover as a space and not on the covering map itself, and it turns out that there is a very nice and quick way to do this.

The idea is the following. Suppose we have a Kirby diagram for $Y = B^4 \setminus \nu F^2$ and a Kirby diagram of its double cover X (which we can produce using Lemma 1.3.8). Now, let $\{h_i^2, h_j^3\}$ be a collection of 2-handles and 3-handles that, when attached to Y, makes us recover B^4. Then,

filling νF into the double cover X simply means attaching lifts of h_i^2 and h_j^3 to X. Hence, if for example h_i^2 is chosen to cancel a 1-handle h^1 of Y, then its lift will cancel a 1-handle lifting of X lifting h^1, because the intersection condition of Proposition 1.2.4 lifts nicely. Similarly, if h_j^3 cancels a 2-handle h^2 of Y, then its lift will cancel a 1-handle of X lifting h^2.

As mentioned above, after this handle cancellation, we usually can no longer see the covering map, but we have a nice simplified Kirby diagram of the double branched cover.

We finish the section and the chapter by computing some useful double branched covers. Consider the unknotted annulus or Möbius band F_n^2:

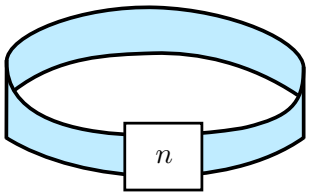

Figure 1.13: The surface F_n^2. The box represents n positive half-twists.

We regard F_n as a properly embedded surface in B^4 by pushing the interior of F_n into the interior of B^4. By realizing the surface as in the left of Figure 1.14, we can easily produce a Kirby diagram of $B^4 \setminus \nu F_n^2$.

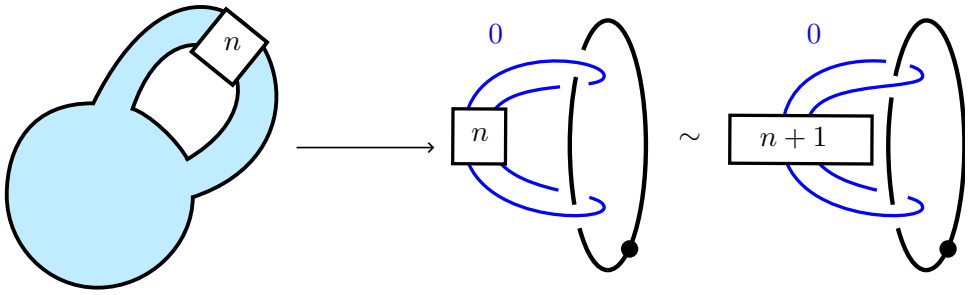

Figure 1.14: The surface F_n^2 (left) and Kirby diagrams of $B^4 \setminus \nu F_n^2$ (right).

Now, using Lemma 1.3.8, we obtain a Kirby diagram of the double cover of $B^4 \setminus \nu F_n^2$. By plugging in $fr(h_Y) = 0, wr(h_X) = 0, wr(h_Y) = -n-1, k = 2$ in Equation 1.1, we obtain the leftmost diagram of Figure 1.15. Now, by attaching a cancelling 2-handle and a cancelling 3-handle to the rightmost diagram of Figure 1.14, we recover B^4. Hence, in order to obtain the double branched cover $\Sigma_2(B^4, F_n^2)$, we simply remove the dotted circle and one of the lifted 2-handles. We thus obtain the Kirby diagram on the right of Figure 1.15.

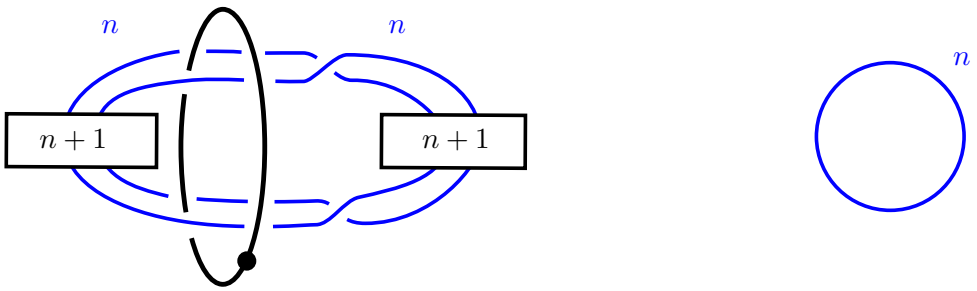

Figure 1.15: Kirby diagram of the double cover of $B^4 \setminus F_n^2$ (left) and of the double branched cover $\Sigma_2(B^4, F_n^2)$ (right).

Chapter 2

Construction of corks

This chapter is devoted to the construction of the corks we will use in the next chapter. We start by defining what a cork is.

Definition 2.0.1. A *cork* is a compact, contractible 4-manifold M, together with a smooth involution $\tau : \partial M \to \partial M$ that does not extend to a diffeomorphism $M \to M$. The involution τ is called the *boundary twist*.

Remark 2.0.2. Freedman proved that any integral homology 3-sphere bounds some compact, contractible, topological 4-manifold W^4. Furthermore, W is unique up to homeomorphism (cf. [2], Section 21.3.2). Since any compact, contractible 4-manifold bounds an integral homology 3-sphere, this implies that the boundary twist $\tau : \partial M \to \partial M$ does extend to a homeomorphism $M \to M$. Hence, the definition of cork already hides some sort of exotic behaviour, so it should not be surprising that they can be used to construct other kinds of exotic phenomena. On the other hand, this suggests that proving that a certain manifold is a cork is a difficult task, as one is supposed to obstruct a map from extending to the interior as a diffeomorphism, but not as a homeomorphism.

Arguably, the most relevant property of corks in the context of low-dimensional topology is that the smooth h-cobordism theorem in dimension 4 is true up to a cork twist. More precisely:

Theorem 2.0.3 ([4])**.** *Let W^5 be a smooth h-cobordism between compact simply-connected manifolds M^4 and N^4. Then, W has a compact contractible sub-h-cobordism K^5 between compact contractible submanifolds $A^4 \subset M^4$ and $B^4 \subset N^4$ so that W is a trivial h-cobordism outside K. In particular, there is a diffeomorphism*

$$W \smallsetminus Int(K) \cong (M \smallsetminus Int(A)) \times [0,1],$$

which induces a diffeomorphism

$$M \smallsetminus Int(A) \overset{F}{\cong} N \smallsetminus Int(B).$$

Furthermore, A and B can be chosen to be diffeomorphic via a diffeomorphism $g : A \to B$ so that the composition $\partial A \overset{g}{\to} \partial B \overset{F}{\to} \partial A$ is an involution.

An immediate consequence of this is the following.

Corollary 2.0.4. *Any exotic pair of simply-connected 4-manifolds is related by a cork twist. That is, the second manifold is obtained by removing a cork from the first one and re-gluing it via its boundary twist.*

The pictures below depict examples of corks (without specifying their boundary twists):

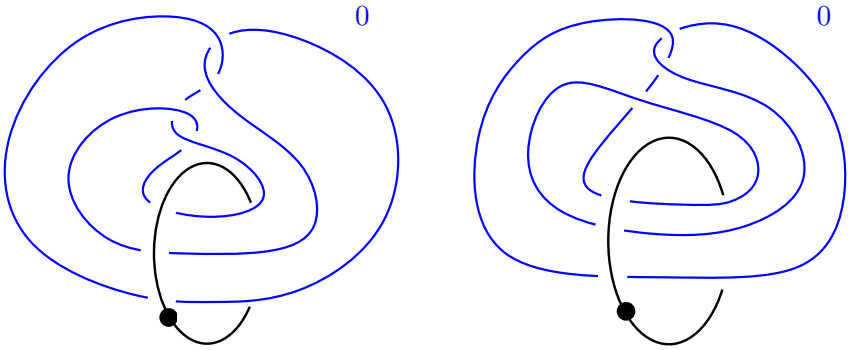

Figure 2.1: (a) the positron and (b) the Mazur cork.

In the next chapter, we will exploit the exotic nature of corks to produce pairs of exotically knotted disks in the 4-ball (relative boundary). However, before getting there, this chapter will deal with the verification that the positron cork above is indeed a cork.

In Section 2.1, we define *contact structures* on 3-manifolds, *Legendrian knots* and their classical invariants. In Section 2.2, we define *Stein domains* and characterize which 4-manifolds admit a structure this kind in terms of their handlebodies. We also state an obstruction for Stein domains that we will use over and over again in the next chapters. Finally, in Section 2.3, we use all of this machinery to prove that the above Kirby diagrams indeed represent corks.

2.1 Contact structures and Legendrian knots

Definition 2.1.1. A *contact structure* on an oriented smooth 3 manifold M is a completely non-integrable oriented 2-plane field ξ. That is, ξ assigns a 2-dimensional subspace ξ_x of T_xM to every point $x \in M$ in a smooth way so that there is no 2-dimensional submanifold whose tangent space at every point x coincides with ξ_x. The pair (M, ξ) is a called a *contact manifold*.

Example 2.1.2. In $\mathbb{R}^3$, the standard contact structure is

$$\xi_{std} = \ker(dz + xdy) = \text{span}\left\{\frac{\partial}{\partial x}, \frac{\partial}{\partial y} - x\frac{\partial}{\partial z}\right\}.$$

Definition 2.1.3. A *contactomorphism* $f : (M_1, \xi_1) \to (M_2, \xi_2)$ between contact manifolds is a diffeomorphism $f : M_1 \to M_2$ so that $\xi_1 = f^*\xi_2$.

Definition 2.1.4. A *Legendrian knot* K in a contact manifold (M^3, ξ) is knot in M that is everywhere tangent to ξ.

Example 2.1.5. Consider the the contact manifold $(\mathbb{R}^3, \xi_{std})$. A knot K in $\mathbb{R}^3$ can be parametrized by a smooth embedding

$$\begin{aligned} \phi : S^1 &\to \mathbb{R}^3 \\ t &\mapsto (x(t), y(t), z(t)), \end{aligned}$$

where we think of S^1 as parametrized by angle $t \in [0, 2\pi]$. In this setting, K is Legendrian if and only if $z'(t) + x(t)y'(t) = 0$ for every $t \in S^1$.

The most common way to picture a Legendrian knot is to take the *front projection* of this parametrization, i.e. project into the yz-plane:

$$\begin{aligned} \phi_\Pi : S^1 &\to \mathbb{R}^2 \\ t &\mapsto (y(t), z(t)). \end{aligned}$$

The x coordinate at each $t \in S^1$ can be recovered using the equation $z'(t) + x(t)y'(t) = 0$ above. Indeed, this implies $x(t) = -\frac{z'(t)}{y'(t)}$. Hence, the front projection of a Legendrian knot, determines the knot itself.

There are two further important features to note about this projection:

(1) It has no vertical tangencies: indeed, a vertical tangency happens whenever $y'(t) = 0$ and $z'(t) \neq 0$, which is impossible by the equation above. However, ϕ must still be an embedding, so if $y'(t) = z'(t) = 0$, then $x'(t) \neq 0$ necessarily. The front projections near these points looks like cusps:

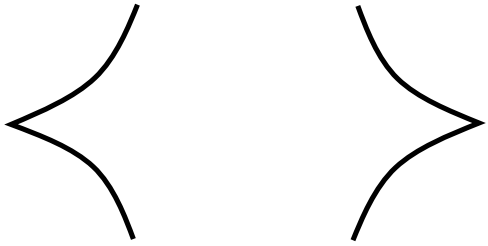

Figure 2.2: Avoiding vertical tangencies

(2) At a double point, the curve that has more slope (i.e. larger $\frac{dz}{dy}$) crosses behind the curve of less slope. Hence, only the crossings on the left of the following figure are allowed:

Figure 2.3: Allowed crossing (left) and forbidden crossing (right)

In Figure 2.4 below there are some examples of front projections of Legendrian knots in $(\mathbb{R}^3, \xi_{std})$.

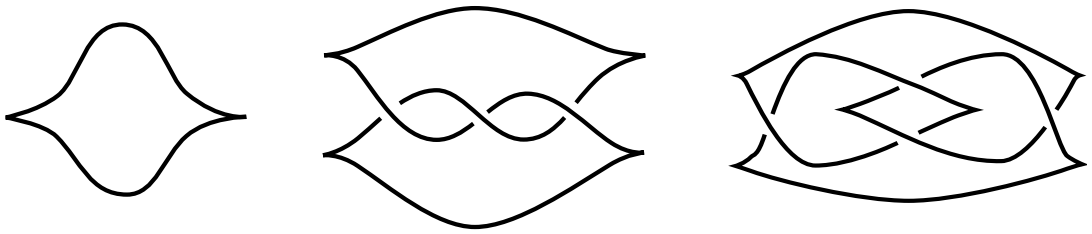

Figure 2.4: Examples of Legendrian knots in $(\mathbb{R}^3, \xi_{std})$: the unknot, the right handed trefoil knot and the figure eight knot, respectively.

It is a standard fact that any smoothly embedded knot admits a projection into $\mathbb{R}^2$ so that self-intersections are transverse and happen at double points. We can further isotope this diagram by replacing each vertical tangency by a left or right cusp (as in Figure 2.2) and any forbidden crossing by either of the following:

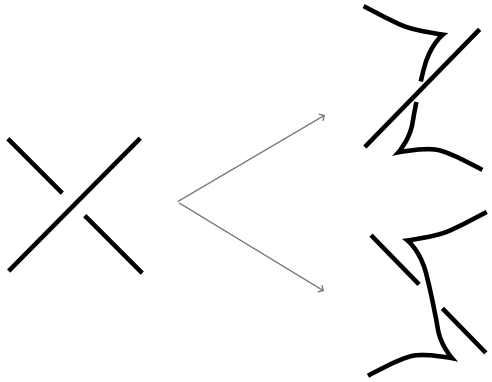

Figure 2.5: Transforming forbidden crossings into allowed ones

Now, such a diagram is the front projection of a Legendrian knot in $(\mathbb{R}^3, \xi_{std})$ by setting $x(t) = -\frac{z'(t)}{y'(t)}$. Thus, we have:

Proposition 2.1.6. *Any smoothly embedded knot in $\mathbb{R}^3$ is smoothly isotopic to a Legendrian knot.*

This example in $\mathbb{R}^3$ is quite representative because by Darboux's theorem ([5]), any two contact manifolds are locally contactomorhic. In particular, any Legendrian knot locally looks like in the example above. Hence, the above proposition is generalized to:

Corollary 2.1.7. *Any smoothly embedded knot in a contact manifold (M^3, ξ) is smoothly isotopic to a Legendrian knot.*

Remark 2.1.8. Everything we have described so far is also true for links.

Next, we want to define a standard contact structure ξ_c on $M_k^3 = \#_k S^1 \times S^2$. By convention, set $M_0^3 = S^3$. Note that M_k^3 is the boundary of $B^4 \cup k$ 1-handles. Hence, it makes sense to draw links in M_k as links in a plane with k dotted circles.

Theorem 2.1.9 ([12])**.** *There exists a contact structure ξ_c on M_k so that any Legendrian link can be pictured in a diagram of the form*

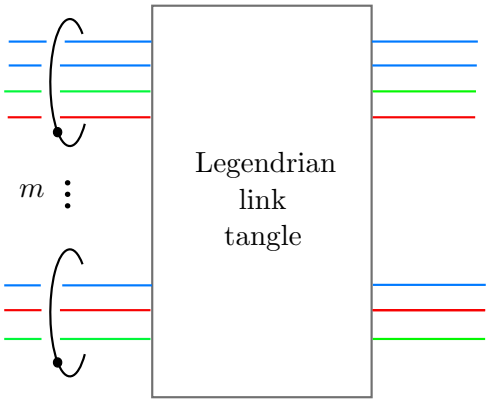

Figure 2.6: Legendrian link diagram in standard form

where:

- *each color represents a component of the link,*
- *the horizontal lines are supposed to be closed above the diagram (just as when taking the closure of a braid). Since this is can be made implicit in the diagram with no ambiguity, we omit these closing lines.*

- *The "Legendrian link tangle" box is a link tangle which is Legendrian in the sense of Example 2.1.5. That means, vertical tangencies are not allowed (they are replaced by cusps) and only crossings on the left of Figure 2.3 are allowed.*

In the next section we will state a more general result (cf. Theorem 2.2.3) which implies the theorem above.

For now, and to finish this section, we define the classical invariants of Legendrian knots. Let K be an oriented Legendrian knot in (M_k, ξ_c).

Definition 2.1.10. The *canonical framing* of K is the framing associated to the normal vector to ξ_c at every point of K. The *Thurston-bennequin number* $tb(K)$ of K is the framing coefficient of its canonical framing. Since this framing differs from the blackboard framing by a left-hand twist for each cusp, it can be computed as

$$tb(K) = wr(K) - \#\text{right cusps}.$$

Definition 2.1.11. The *rotation number* of K is

$$r(K) = \#\text{downward left cusps} - \#\text{upward right cusps}.$$

For an intrinsic definition of this invariant, see [8] §2.6 or [14] §11.1.

Example 2.1.12. The knots of Figure 2.4 have $(tb, r) = (-1, 0)$, $(tb, r) = (1, 0)$, $(tb, r) = (-3, 0)$, respectively.

Remark 2.1.13. Note that these numbers are not invariant up to smooth (or topological) isotopy. However, they are invariant up to Legendrian isotopy.

2.2 Stein domains

In this section we define a family of 4-manifolds with some extra structure that induces a contact structure on their boundary. These manifolds are called *Stein domains*. After this, we give a simple characterization of them in terms of handlebody decompositions. Lastly, we state three obstruction inequalities about these manifolds that will be used in the next sections.

Let W^4 be a complex surface with boundary. Then, its complex structure J induces a 2-plane field on its boundary M^3 via

$$\xi_x = T_x M \cap J(T_x M).$$

However, this ξ need not define a contact structure on M^3. The next definition imposes some extra structure making sure that the 2-plane field above does define a contact structure.

Definition 2.2.1. A complex surface W^4 with boundary is a *Stein domain* if it admits a proper Morse function $f : W^4 \to [0, 1]$ with $\partial W = f^{-1}(1)$ and such that, away from the critical points, the complex structure induces a contact structure on each level set $f^{-1}(t)$.

Example 2.2.2 ([12]). The 4-ball $B^4 \subset \mathbb{C}^2$ with the Morse function $\phi(z) = ||z||^2$ is a Stein domain. Let ξ_c be the contact structure induced on $S^3 = \partial B^4$. Then, $(S^3 \setminus *, \xi_c)$ and $(\mathbb{R}^3, \xi_{std})$ are contactomorphic. In particular, this proves Theorem 2.1.9 for $k = 0$.

Further examples of Stein domains will be constructed using the following results:

Theorem 2.2.3. *([7]) A 4-manifold consisting of one 0-handle and k 1-handles admits the structure of a Stein domain whose induced contact structure on the boundary is (contactomorphic to) ξ_c from Theorem 2.1.9.*

Theorem 2.2.4. *([7], [12]) Suppose W^4 admits a handle decomposition of the form*

$$W = h^0 \cup h^1_1 \cup \ldots \cup h^1_k \cup h^2_1 \cup \ldots \cup h^2_l.$$

Denote $W_1 = h^0 \cup h^1_1 \cup \ldots \cup h^1_k$ and consider the contact structure ξ_c on its boundary $\partial W_1 \cong \#_k S^1 \times S^2$ given by Theorem 2.2.3. Suppose that every 2-handle h^2_i is attached to ∂W_1 along a Legendrian knot K_i with framing $tb(K_i) - 1$. Then, W admits the structure of a Stein domain such that the Chern class $c_1(W)$ is represented by a cocycle φ with $\langle \varphi, h^2_i \rangle = r(K_i)$ after orienting K_i. Moreover, Legendrian knots in ∂W can still be pictured by diagrams in standard form (i.e. as in Figure 2.6).

To end this section, we state three obstruction inequalities for Stein domains. They all follow from an adjunction inequality from Seiberg-Witten theory.

Theorem 2.2.5. *([20], Theorem 3.4) Let W^4 be a Stein domain with $M^3 = \partial W$. Let K be a Legendrian knot in M. Then:*

$$tb(K) + |r(K)| \leq 2g_4(K) - 1,$$

where $g_4(K)$ is the minimal genus of a surface in W that bounds K.

Theorem 2.2.6. *([20], Proposition 2.1) Let W^4 be a Stein domain and S a smoothly embedded orientable surface in W with $g(S) > 0$ and $[S]^2 \geq 0$. Then:*

$$[S]^2 + |\langle c_1(W), [S] \rangle| \leq 2g(S) - 2.$$

Along a similar line, we have a statement for smoothly embedded 2-spheres.

Theorem 2.2.7. *([20], Proposition 2.2) Let W^4 be a Stein domain and S a smoothly embedded 2-sphere in W with $[S] \neq 0$ in $H_2(W)$. Then, $[S]^2 \leq -2$ and if equality holds, then $\langle c_1(W), [S] \rangle = 0$.*

This last result will be the most important obstruction in this work, as almost every construction we make will rely on it.

2.3 Examples of corks

In this section we prove that the positron cork is indeed a cork. An analogous argument works also for the Mazur cork.

Denote the positron cork of Figure 2.1 by W^4. First we define its boundary twist. Its Kirby diagram can be isotoped to look like in Figure 2.7 below. This picture has the advantage of being symmetric with respect to the vertical axis. Furthermore, the boundary of a 4-manifold does not distinguish between carving out the tubular neighborhood of a disk (i.e. a dotted circle) and attaching a 0-framed 2-handle along an unknot.[1] Hence, we can swap the dotted circle by the 0-framed unknot giving an involution τ of the boundary ∂W.

[1] In fact, both of them yield, on the boundary, 0-framed Dehn surgery along the unknot.

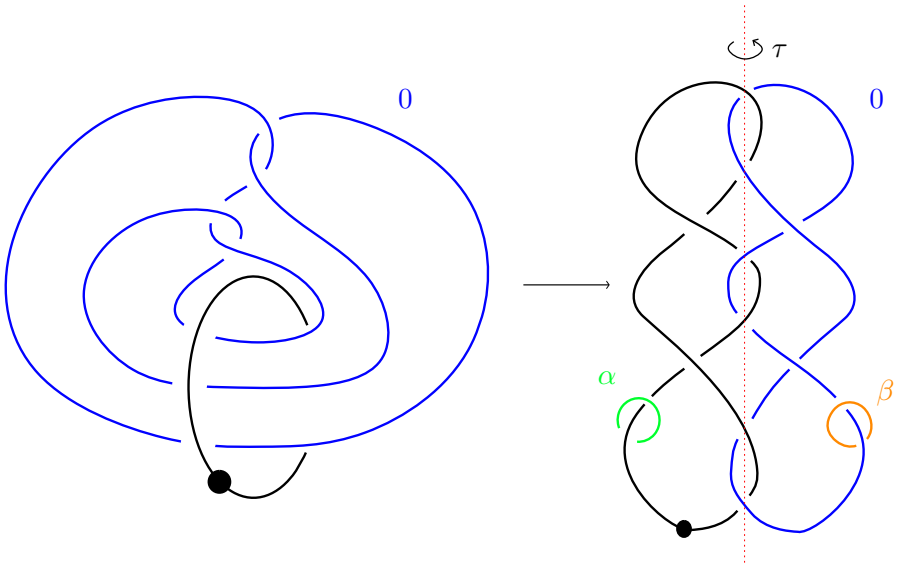

Figure 2.7: The positron cork W^4 and its boundary twist $\tau : \partial W \to \partial W$.

Claim 2.3.1. *W^4 is compact and contractible.*

Proof. Compactness is clear because W^4 is defined by a Kirby diagram with a finite number of handles. In order to show that W^4 is contractible, note that the homotopy type of a manifold after attaching a k-handle on the homotopy class of its attaching sphere. This is because handlebodies are just CW complexes with thickened cells, and the homotopy type of a CW complex depends only on the homotopy class of its attaching maps ([16], Proposition 0.18). This means in particular that in an Kirby diagram we are free to reverse any crossing of the attaching sphere of a 2-handle. Hence, we have a chain of homotopy equivalences:

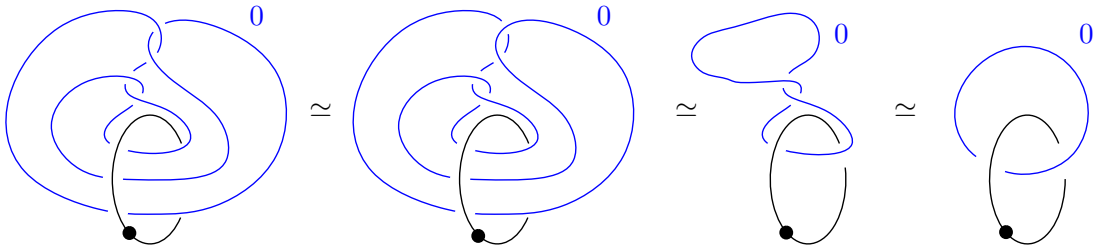

Figure 2.8: The positron cork is contractible.

The last Kirby diagram in the figure above is a cancelling pair, so it is the 4-ball, and hence contractible. □

It remains to show that the involution $\tau : \partial W \to \partial W$ does not extend to a diffeomorphism $W \to W$. Note that τ sends the knot α to the knot β (cf. Figure 2.7). Since the knot β goes around the attaching sphere of the 2-handle, it is (smoothly) slice. A slice disk can be seen as the obvious one by pushing its interior into the interior of W^4. Now, if τ did extend to the interior, then α would also be slice, so it suffices to prove that this is not the case. In order to do this, we will use the obstruction on the 4-genus of a knot given in Theorem 2.2.5.

Claim 2.3.2. *W^4 is a Stein domain.*

Proof. The leftmost Kirby diagram of Figure 2.1 can be pictured in standard form as in Figure 2.9 below.

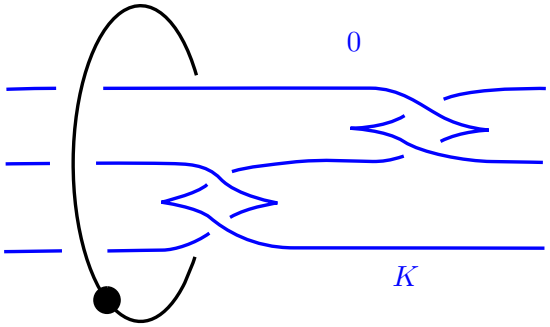

Figure 2.9: Kirby diagram of the positron cork in standard form.

The 2-handle is attached along a Legendrian knot K with $tb(K) = 4 - 2 = 2$. Hence, the framing is not $tb(K) - 1$, as Theorem 2.2.4 requires. However, the Thurston-Bennequin number of a Legendrian knot can be made as small as we want without changing its smooth isotopy class. This is done in Figure 2.10 by adding a right and a left cusp.

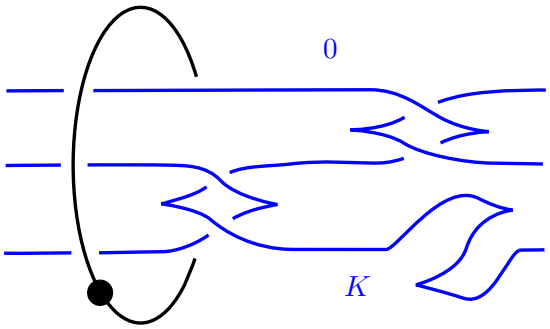

Figure 2.10: Kirby diagram of the positron cork as a Stein domain.

Now, the framing of the 2-handle equals $0 = tb(K) - 1$, so we are in the situation of Theorem 2.2.4. Hence, W^4 is a Stein domain. □

Claim 2.3.3. *The knot α is not slice.*

Proof. From the picture below we have $tb(\alpha) = 0$ and $r(\alpha) = 0$ so Theorem 2.2.5 implies $0 \leq 2g_4(\alpha) - 1$ and hence $g_4(\alpha) > 0$, so α is not slice.

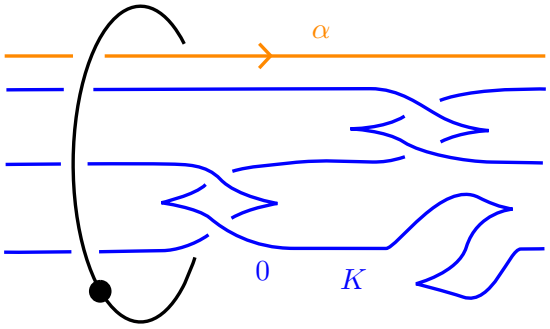

Figure 2.11: The positron cork and the knot α in standard form.

□

Remark 2.3.4. By Remark 2.0.2, τ does extend to a homeomorphism $W \to W$, so α is topologically slice. In particular, this shows the existence of knots that are topologically slice, but not smoothly slice, although they live in the non-trivial integral homology 3-sphere ∂W.

Chapter 3

Exotically knotted complex curves in $\mathbb{C}^2$

The ultimate goal of this chapter is to present Hayden's argument for proving:

Theorem A. *There exist infinitely many pairs of proper holomorphic complex curves in $\mathbb{C}^2$ which are exotically knotted.*

In Section 3.1, we exploit the cork's exotic nature to produce exotically knotted disks in B^4 (relative boundary). This step is actually not necessary towards proving the theorem above, but the idea of distinguishing double branched covers to obstruct surfaces from being isotopic will be used over and over again in the next sections.

In Section 3.2, we go several steps ahead and produce surfaces of any positive genus which are exotically knotted in B^4 and remain exotically knotted when restricted to the interiors.

In Section 3.3, we realize the surfaces above as positively braided surfaces and consequently as compact pieces of complex algebraic curves.

Finally, in Section 3.4 we find a Fatou-Bieberbach domain that allows us to holomorphically embed the interior of these compact pieces into $\mathbb{C}^2$ while retaining the exotic behaviour proven in Section 3.2.

3.1 Exotically knotted disks in B^4

In this section, we produce a pair of properly embedded disks in B^4 which are exotically knotted relative boundary. These disks will constitute the fundamental building blocks for every construction in this work. In the next chapter, we will be able to extend this result to arbitrarily large n-tuples of exotically knotted disks relative boundary (cf. Theorem D).

Consider the ribbon disks D and D' of Figure 3.1 below that bound the knot $K = 17nh_{74}$.

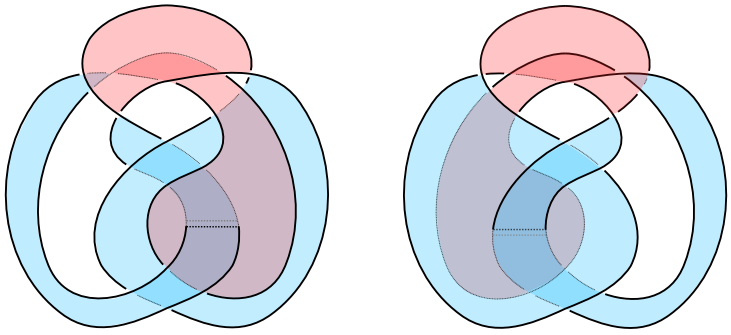

Figure 3.1: The disks D (left) and D' (right).

Notice that they are clearly smoothly isotopic, as D' is obtained from D by rotating it 180^o along the vertical axis. However, since they have the same boundary $K = \partial D = \partial D'$, it still makes sense to ask whether they are topologically or smoothly isotopic relative boundary.

We first deal with the topological isotopy. This will be a consequence of a result proven by Conway and Powell (namely Theorem 3.1.3 below). In order to match their conventions, we first give some general definitions.

Definition 3.1.1. Let $D \subset B^4$ be a (topologically) slice disk for a knot K in S^3. We say that D is *homotopy ribbon* if the inclusion map $S^3 \setminus \nu K \hookrightarrow B^4 \setminus \nu D$ induces a surjection $\pi_1(S^3 \setminus \nu K) \twoheadrightarrow \pi_1(B^4 \setminus \nu D)$. The knot K is called *homotopy ribbon* if it bounds a homotopy ribbon disk.

Definition 3.1.2. Let G be a group. A homotopy ribbon disk D is called *G-homotopy ribbon* if $\pi_1(B^4 \setminus \nu D) \cong G$. An oriented knot is called *G-homotopy ribbon* if it bounds a G-homotopy ribbon disk.

This already allows us to state the result we are interested in:

Theorem 3.1.3 ([3])**.** *Any two $\mathbb{Z}$-homotopy ribbon disks for the same $\mathbb{Z}$-homotopy ribbon knot are ambiently topologically isotopic relative boundary.*

We will rather use this in the following form:

Corollary 3.1.4. *Let D and D' be two smooth, properly embedded disks in B^4 with $K = \partial D = \partial D'$. If $\pi_1(B^4 \setminus D) \cong \pi_1(B^4 \setminus D') \cong \mathbb{Z}$, then the disks are ambiently topologically isotopic relative boundary.*

Proof. By the preceding theorem, it suffices to show that D is a homotopy ribbon disk (the argument for D' is, of course, exactly the same). Hence, we want to show that the inclusion induced homomorphism $\pi_1(S^3 \setminus \nu K) \twoheadrightarrow \pi_1(B^4 \setminus \nu D)$ is surjective. For this, since $\pi_1(B^4 \setminus \nu D) \cong \mathbb{Z}$, it will be enough to prove that the corresponding homomorphism on abelianizations $H_1(S^3 \setminus \nu K) \twoheadrightarrow H_1(B^4 \setminus \nu D)$ is surjective (integer coefficients are assumed unless otherwise stated). The Mayer-Vietoris sequences associated to the decompositions $S^3 = (S^3 \setminus K) \cup \nu K$, $B^4 = (B^4 \setminus D) \cup \nu D$ fit into a commutative diagram with exact rows:

$$\begin{array}{ccccccccc}
H_2(S^3) & \longrightarrow & H_1(\nu K \setminus K) & \longrightarrow & H_1(S^3 \setminus K) \oplus H_1(\nu K) & \longrightarrow & H_1(S^3) & \longrightarrow & \tilde{H}_0(\nu K \setminus K) \\
\downarrow & & \downarrow & & \downarrow & & \downarrow & & \downarrow \\
H_2(B^4) & \longrightarrow & H_1(\nu D \setminus D) & \longrightarrow & H_1(B^4 \setminus D) \oplus H_1(\nu D) & \longrightarrow & H_1(B^4) & \longrightarrow & \tilde{H}_0(\nu D \setminus D)
\end{array}$$

Plugging in the known values of the groups, we get:

$$\begin{array}{ccccccccc}
0 & \longrightarrow & H_1(K \times S^1) & \longrightarrow & H_1(S^3 \setminus K) \oplus H_1(K) & \longrightarrow & 0 & \longrightarrow & 0 \\
\downarrow & & \downarrow\!\!\downarrow & & \downarrow & & \downarrow & & \downarrow \\
0 & \longrightarrow & H_1(D \times S^1) & \longrightarrow & H_1(B^4 \setminus D) \oplus 0 & \longrightarrow & 0 & \longrightarrow & 0
\end{array}$$

Notice that the second vertical map starting from the left is surjective, as $H_1(D \times S^1)$ is generated by $\{*\} \times S^1$. By the 5-Lemma, the middle arrow is also surjective. But notice that it sends $H_1(K)$ to $H_1(D) = 0$. Hence, the map $H_1(S^3 \setminus K) \to H_1(B^4 \setminus D)$ is surjective. □

This last result easily allows us to confirm:

Corollary 3.1.5. *The disks D and D' of Figure 3.1 are topologically isotopic relative boundary.*

Proof. By Corollary 3.1.4 above, it suffices to show $\pi_1(B^4 \smallsetminus D) \cong \pi_1(B^4 \smallsetminus D') \cong \mathbb{Z}$. In fact, it is enough to prove this for D, as D and D' are clearly isotopic (via the obvious isotopy that does not preserve the boundary). Following [14], §6.2, we produce a Kirby diagram of $B^4 \smallsetminus \nu D$ (middle of Figure 3.2). We could already compute the fundamental group using this diagram and Proposition 1.2.5, but for later purposes it will be convenient to perform a 1-handle slide first. This way, we obtain the rightmost diagram of Figure 3.2.

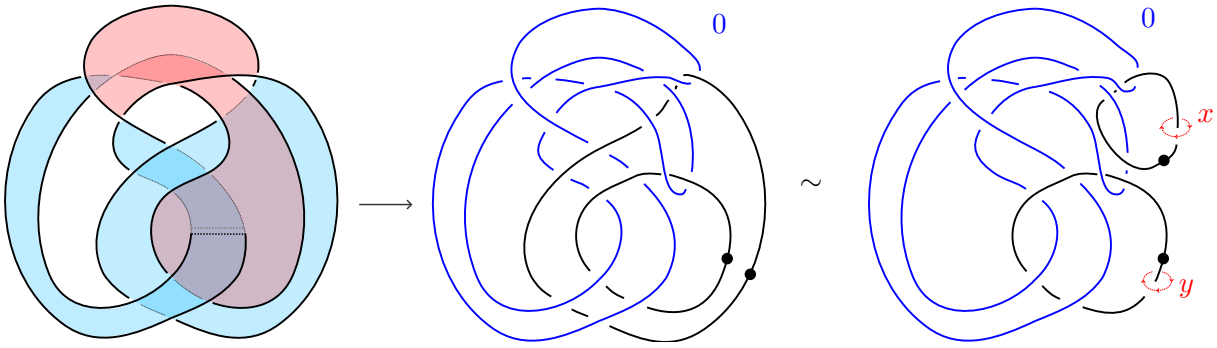

Figure 3.2: The complement $B^4 \smallsetminus \nu D$.

Now, using Proposition 1.2.5, we obtain

$$\pi_1(B^4 \smallsetminus \nu D) \cong \langle x, y | xy^{-1}yx^{-1}y \rangle \cong \langle x, y | y = 1 \rangle \cong \mathbb{Z},$$

as wanted. □

In order to prove that the disks D and D' are not smoohtly isotopic relative boundary, we will realize the double branched cover $\Sigma_2(B^4, D)$ as the positron cork and then exploit its boundary twist to obstruct the smooth isotopy. The first part is stated in the following lemma and proven in the appendix.

Lemma A.1. *A Kirby diagram of the double branched cover $\Sigma_2(B^4, D)$ is shown on the right of Figure 3.3. Furthermore, the loops γ and γ' on the left, have lifts $\tilde{\gamma}$ and $\tilde{\gamma}'$, respectively.*

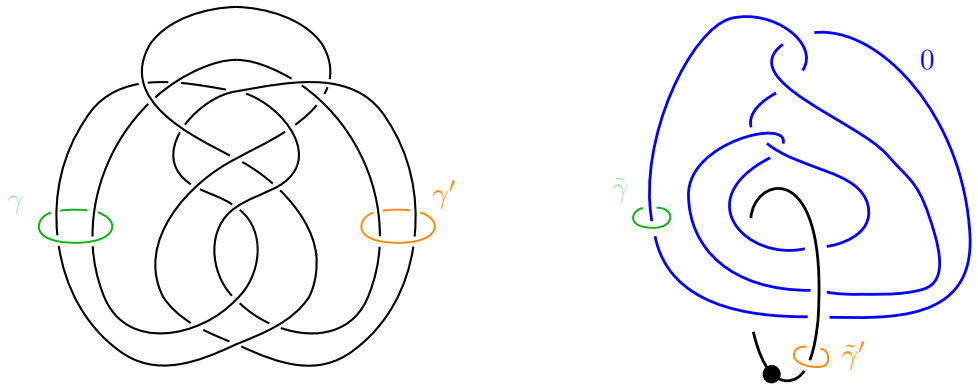

Figure 3.3: The knot K together with two loops γ and γ' (left). The double branched cover $\Sigma_2(B^4, D)$ together with lifts of γ and γ' (right).

We are now ready to prove:

Theorem B. *The disks D and D' of Figure 3.1 are exotically knotted relative boundary.*

Proof. We only need to check that they are not smoothly isotopic relative boundary. Suppose they are, i.e. we have a diffeomorphism $\varphi : (B^4, D) \to (B^4, D')$ that preserves the boundary pointwise. Consider also the obvious involution $\eta : B^4 \to B^4$ which maps D to D'. Notice that η sends γ to γ' (See Figure 3.3 above).

Thus, the composition $\eta \circ \varphi$ defines a diffeomorphism $(B^4, D) \to (B^4, D)$ which sends γ to γ'. By lifting to double branched covers, we get a commutative diagram:

$$\begin{array}{ccccc}
\tilde{\gamma} & \longmapsto & & & \tilde{\gamma}' \\
\\
\Sigma_2(B^4, D) & & \xrightarrow{\cong} & & \Sigma_2(B^4, D) \\
\downarrow & & & & \downarrow \\
(B^4, D) & \xrightarrow{\varphi} & (B^4, D') & \xrightarrow{\eta} & (B^4, D) \\
\\
\gamma & & \longmapsto & & \gamma'
\end{array}$$

In particular, we have obtained a self-diffeomorphism of $\Sigma_2(B^4, D)$ which sends $\tilde{\gamma}$ to $\tilde{\gamma}'$, which contradicts Claim 2.3.3 (essentially the fact that the cork's boundary twist does not extend to the interior). □

3.2 Exotically knotted surfaces in $\mathring{B}^4$

In this section we go several steps ahead and construct pairs of exotically knotted surfaces in B^4 of arbitrary genus and number of holes (except for the disk). Crucially for the next sections, these pairs of surfaces will remain exotically knotted when restricted to the interior of the 4-ball. The argument we present resembles the one of the previous section in the sense that in order to distinguish the smooth isotopy classes of two surfaces, we distinguish the double branched covers along them. This time, however, the obstruction we use will be Theorem 2.2.7. In particular, this justifies that this argument does not work for the disks, as $H_2(\Sigma_2(B^4, D)) = 0$.

We start with the annuli and once punctured tori of Figures 3.4 and 3.5.

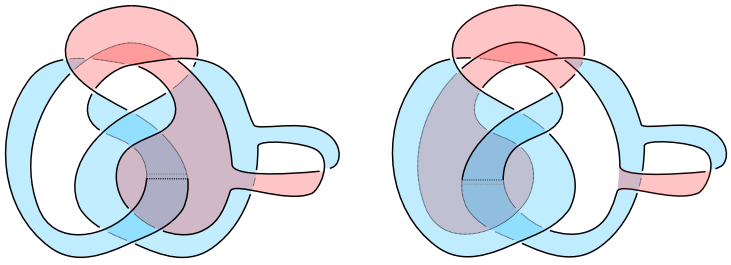

Figure 3.4: The annuli A (left) and A' (right).

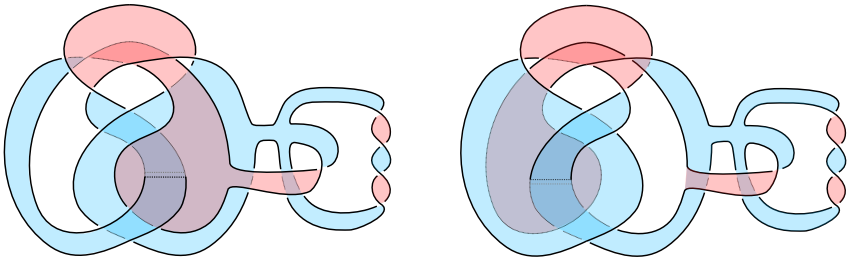

Figure 3.5: The tori T (left) and T' (right).

Notice that both pairs of surfaces are topologically isotopic relative boundary. Indeed, they are obtained by attaching the same bands in the same manner to the boundary $K = \partial D = \partial D'$, so we can simply extend the topological isotopy relative boundary between D and D'.

The proof that they are not smoothly isotopic will consist of the following two steps.

Proposition 3.2.1. *The double branched covers $\Sigma_2(B^4, A')$ and $\Sigma_2(B^4, T')$ contain smoothly embedded 2-spheres of self-intersection number -2.*

Proposition 3.2.2. *The double branched covers $\Sigma_2(B^4, A)$ and $\Sigma_2(B^4, T)$ do not contain smoothly embedded 2-spheres of self-intersection number -2.*

Notice that this will prove something stronger. Namely, that the pairs (B^4, A) and (B^4, A') are not diffeomorphic (and likewise for the tori). Let's begin by explicitly constructing these 2-spheres.

Proof. (of 3.2.1) By Lemma A.3 in the Appendix, these spheres can be realized by the Seifert disks of the purple 2-handle with interior pushed into the interior of the 4-manifold and capping them off with the core of the 2-handle (cf. Proposition 1.2.10). □

In order to prove Proposition 3.2.2, we first compute Kirby diagrams for $\Sigma_2(B^4, A)$ and $\Sigma_2(B^4, T)$.

Lemma A.2. *The following are Kirby diagrams for the double branched covers $\Sigma_2(B^4, A)$ and $\Sigma_2(B^4, T)$, respectively.*

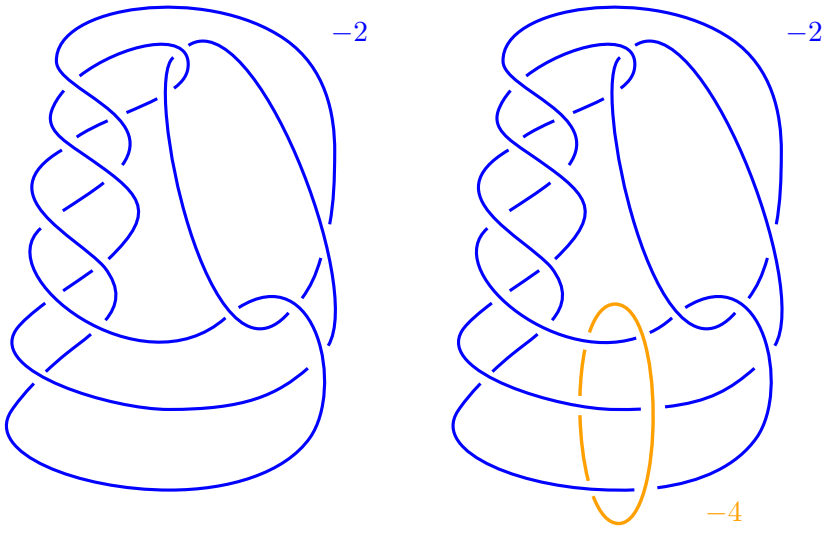

Figure 3.6: Kirby diagrams of $\Sigma_2(B^4, A)$ (left) and $\Sigma_2(B^4, T)$ (right).

We are now ready to prove Proposition 3.2.2. We will use the genus obstruction from Theorem 2.2.7.

Proof. (of 3.2.2) The Kirby diagrams of Figure 3.6 can be redrawn in standard form:

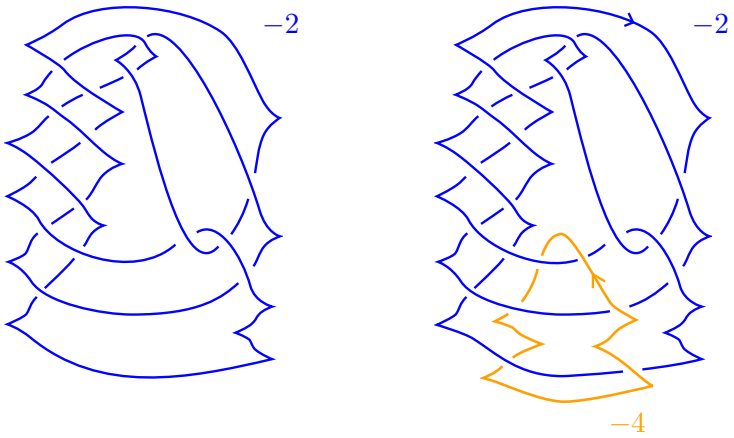

Figure 3.7: Kirby diagrams for $\Sigma_2(B^4, A)$ (left) and $\Sigma_2(B^4, T)$ (right) in standard form.

Let us call K_1 the blue knot and K_2 the orange one with the orientations given above. Let $W_A = \Sigma_2(B^4, A)$ and $W_T = \Sigma_2(B^4, T)$. We have $tb(K_1) = -1, r(K_1) = -2, tb(K_2) = -3, r(K_2) = 0$. By Theorem 2.2.4, both W_A and W_T admit Stein structures so that their Chern classes satisfy

$$\langle c_1(W_A), h_1\rangle = \langle c_1(W_T), h_1\rangle = r(K_1) = -2,$$

where h_1 is the homology class represented by the blue 2-handle in each case. Now, suppose S is a smoothly embedded 2-sphere in W_A with $[S]^2 = -2$. In particular, $[S] = \lambda h$ for some non-zero $\lambda \in \mathbb{Z}$. Hence, $\langle c_1(W_A), [S]\rangle = \lambda\langle c_1(W_A), h_1\rangle = -2\lambda \neq 0$, contradicting Theorem 2.2.7.

The argument for W_T is essentially the same. Suppose S is a smoothly embedded 2-sphere in W_T with $[S]^2 = -2$. The intersection form of W_T with respect to the basis $\{h_1, h_2\}$ of $H_2(W_T)$ has matrix (cf. Proposition 1.2.10)

$$\begin{bmatrix} -2 & 1 \\ 1 & -4 \end{bmatrix}$$

Writing $[S] = \lambda h_1 + \mu h_2$ and setting $[S]^2 = -2$, we obtain

$$-2 = \begin{bmatrix} \lambda & \mu \end{bmatrix} \begin{bmatrix} -2 & 1 \\ 1 & -4 \end{bmatrix} \begin{bmatrix} \lambda \\ \mu \end{bmatrix} = -2(\lambda^2 - \lambda\mu + 2\mu^2)$$

Hence, we must have $\lambda^2 - \lambda\mu + 2\mu^2 = 1$, which has a unique integer solution up to sign: $\lambda = \pm 1$, $\mu = 0$. This implies $\langle c_1(W_T), [S]\rangle = \mp 2 \neq 0$, contradicting Theorem 2.2.7 again. □

The next step is to extend this construction to pairs of exotically knotted orientable surfaces with boundary of arbitrary genus and number of holes. Notice that the classical classification theorem for closed smooth (or topological) surfaces immediately implies:

Theorem 3.2.3. *(Classification of compact surfaces with boundary) Let S be a compact, connected, topological (resp. smooth) surface with boundary. Suppose its boundary has k components. Then, S is homeomorphic (resp. diffeomorphic) to X-with-k-holes, where X is exactly one of the following:*

(1) S^2,

(2) $\#_m T^2$, *or*

(3) $\#_m P^2$.

(1) and (2) are orientable and (3) is not.

We will be interested in writing these surfaces as boundary connected sums of simple pieces. For this, let A_1 be S^2-with-2-holes (i.e. an annulus), T_1 be T^2-with-1-hole, and M_1 be P^2-with-1-hole (i.e. a Möbius band). We can reformulate the above theorem as:

Corollary 3.2.4. *Any compact, connected, topological (resp. smooth) surface with boundary is homeomorphic (resp. diffeomorphic) to exactly one of the following:*

(1) the disk D^2,

(2) $\natural_k A_1$ with $k \geq 1$,

(3) $\natural_k A_1 \natural_m T_1$ with $k \geq 0, m \geq 1$, or

(4) $\natural_k A_1 \natural_m M_1$ with $k \geq 0, m \geq 1$.

(1), (2) and (3) are orientable and (4) is not.

Fortunately for us, double branched covers behave very nicely under boundary connected sums. Namely:

Proposition 3.2.5. *Let S_1 and S_2 be two smooth, properly embedded, compact, connected surfaces in B^4. Then, we have a diffeomorphism*

$$\Sigma_2(B^4, S_1 \natural S_2) \cong \Sigma_2(B^4, S_1) \natural \Sigma_2(B^4, S_2).$$

Proof. Realize the branching action in the 4-dimensional 1-handle $D^1 \times D^3$ along $D^1 \times D^1 \subset D^1 \times D^3$ by squaring around the axis D^1 of D^3. Glue the 4-manifolds $\Sigma_2(B^4, S_1)$ and $\Sigma_2(B^4, S_2)$ with such a 1-handle to obtain $\Sigma_2(B^4, S_1) \natural \Sigma_2(B^4, S_2)$. By our choice of gluing, this clearly covers B^4 branched along $S_1 \natural S_2$. Finally, by uniqueness of double branched covers (cf. Proposition 1.3.6) we get the diffeomorphism. □

Remark 3.2.6. The embedded boundary connected sum of two embedded surfaces is of course not well-defined (for example, when one of the surfaces has boundary with several connected components). However, this will not matter for our argument, as the only crucial thing is that we boundary sum pairs of topologically isotopic surfaces (relative boundary) using the same embedded bands, so that the resulting embedded surfaces are still topologically isotopic relative boundary.

By Corollary 3.2.4, in order to obtain orientable surfaces with more holes and more genus, we will need to boundary sum annuli and tori-with-1-hole. More explicitly, consider the annulus A_0 and torus-with-1-hole T_0 of the Figure below:

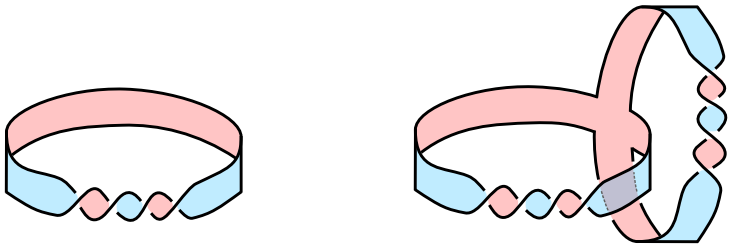

Figure 3.8: The annulus A_0 (left) and the torus-with-1-hole T_0 (right)

By the final part of Section 1.3, the double branched covers of B^4 along these surfaces have Kirby diagrams:

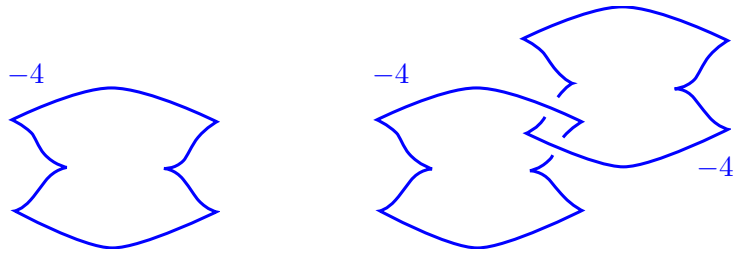

Figure 3.9: Kirby diagrams of $\Sigma_2(B^4, A_0)$ (left) and of $\Sigma_2(B^4, T_0)$ in standard form.

In particular, notice that they admit structures of Stein domains (cf. Theorem 2.2.4).

We are now ready to prove:

Theorem C. *Any compact, connected, orientable surface with boundary (other than the disk) admits a pair of smooth, proper embeddings in B^4 that are exotically knotted. Furthermore, they remain exotically knotted when restricted to the interior.*

Proof. By Corollary 3.2.4, such surface will be diffeomorphic to $\natural_k A_1$ with $k \geq 1$, or to $\natural_k A_1 \natural_m T_1$ with $k \geq 0, m \geq 1$. Let us start with the first case.

Pick $F = A \natural_{k-1} A_0$ and $F' = A' \natural_{k-1} A_0$. Notice that by boundary summing in the same manner in each case, these surfaces will be topologically isotopic relative boundary, because their summands were. Denote the double branched covers $\Sigma_2(B^4, F)$ and $\Sigma_2(B^4, F')$ by W and W', respectively. By Proposition 3.2.5, we have diffeomorphisms

$$W \cong \Sigma_2(B^4, A) \natural_{k-1} \Sigma_2(B^4, A_0),$$
$$W' \cong \Sigma_2(B^4, A') \natural_{k-1} \Sigma_2(B^4, A_0).$$

Since $\Sigma_2(B^4, A')$ contains a smoothly embedded 2-sphere of square -2, so will W'. It suffices to show that W does not contain such sphere. Notice that a Kirby diagram of W can be obtained by drawing Kirby diagrams of its boundary connected summands side by side. Since all of these Kirby diagrams have the right relation between framing coefficients and Thurston-Bennequin numbers, Theorem 2.2.4 implies that W admits a Stein structure with $\langle c_1(W), h_1 \rangle = -2$, where h_1 is the homology class associated to the 2-handle of $\Sigma_2(B^4, A)$ of Figure 3.7. Now, with respect to the basis $\{h_1, \ldots, h_k\}$ of $H_2(W)$ associated to the 2-handles the intersection form of W has the block-sum matrix (cf. Proposition 1.2.10)

$$[-2] \oplus_{k-1} [-4].$$

Suppose S is a smoothly embedded 2-sphere in W with $[S]^2 = -2$. Then, $[S] = \pm h_1$ and hence $\langle c_1(W), [S] \rangle = \mp 2 \neq 0$, contradicting Theorem 2.2.7.

For the second case, pick $F = T \natural_k A_0 \natural_{m-1} T_0$ and $F' = T' \natural_k A_0 \natural_{m-1} T_0$. Again, denote the double branched covers along these surfaces by W and W', respectively. We have diffeomorphisms

$$W \cong \Sigma_2(B^4, T) \natural_k \Sigma_2(B^4, A_0) \natural_{m-1} \Sigma_2(B^4, T_0),$$
$$W' \cong \Sigma_2(B^4, T') \natural_k \Sigma_2(B^4, A_0) \natural_{m-1} \Sigma_2(B^4, T_0).$$

Since $\Sigma_2(B^4, T')$ contains a smoothly embedded 2-sphere of square -2, so will W'. As before, it suffices to show that W does not contain such sphere. Again, W will admit a Stein structure with $\langle c_1(W), h_1 \rangle = -2$. With respect to the basis $\{h_1, h_2, b_i, c_j, d_j\}$ of $H_2(W)$ represented by the 2-handles, the intersection form of W has the block-sum matrix

$$\begin{bmatrix} -2 & 1 \\ 1 & -4 \end{bmatrix} \oplus_k [-4] \oplus_{m-1} \begin{bmatrix} -4 & 1 \\ 1 & -4 \end{bmatrix}$$

Now, suppose S is a smoothly embedded 2-sphere in W with $[S]^2 = -2$. Notice that the matrices $A = \begin{bmatrix} -2 & 1 \\ 1 & -4 \end{bmatrix}$ $B = [-4]$ and $C = \begin{bmatrix} -4 & 1 \\ 1 & -4 \end{bmatrix}$ satisfy $v^T Av \leq -2$, $v^T Bv, v^T Cv < -2$ for every vector $v \neq 0$ with integer coefficients. This is because $A + 2id$ is negative semi-definite and both $B + 2id$ and $C + 2id$ are negative definite. Hence, the equation $[S]^2 = -2$ implies $[S] = \pm h_1$, so $\langle c_1(W), [S] \rangle = \mp 2 \neq 0$, contradicting Theorem 2.2.7.

Notice that in each case we have distinguished the interiors of the double branched covers. Hence, the surfaces remain exotically knotted when restricted to the interior. □

3.3 Braided surfaces and algebraic curves

The goal of this section is to realize the previous surfaces as compact pieces of algebraic curves. Namely, we prove:

Theorem 3.3.1. *Fix the topological type $\mathcal{F}$ of any compact, connected, orientable surface with boundary other than the disk. Let $\mathbb{D}$ denote the unit bidisk $D^2 \times D^2$. There exist complex algebraic curves $V_0, V_1 \subset \mathbb{C}^2$ so that*

(i) the intersections $F_0 = V_0 \cap \mathbb{D}$, $F_1 = V_1 \cap \mathbb{D}$ have topological type $\mathcal{F}$ and are properly embedded in $\mathbb{D}$,

(ii) F_0 and F_1 are isotopic through homeomorphisms of $\mathbb{D}$ that are smooth in a neighborhood of $\partial\mathbb{D}$,

(iii) the intermediate surfaces F_t of the isotopy have boundary in $\partial D^2 \times \mathring{D}^2$,

(iv) $\Sigma_2(\mathbb{D}, F_0)$ contains a smoothly embedded 2-sphere of square -2, and

(v) $\Sigma_2(\mathbb{D}, F_1)$ does not contain a smoothly embedded 2-sphere of square -2.

Before we get into the details, we introduce braided surfaces.

Definition 3.3.2. The *n-stranded braid group* B_n is

$$\langle \sigma_1, \ldots, \sigma_{n-1} | \sigma_i \sigma_{i+1} \sigma_i = \sigma_{i+1} \sigma_i \sigma_{i+1}, \sigma_i \sigma_j = \sigma_j \sigma_i, \text{ for } |i-j| \geq 2 \rangle.$$

The generators $\sigma_1, \ldots, \sigma_{n-1}$ are called *Artin generators*.

Recall that any element in B_n can be geometrically realized by an n-braid. For example, the Artin generators are realized as the n-braids (for $n = 3$)

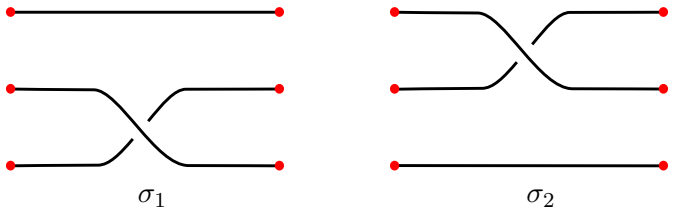

Figure 3.10: The Artin generators of B_3.

We can also realize their inverses by changing the crossings:

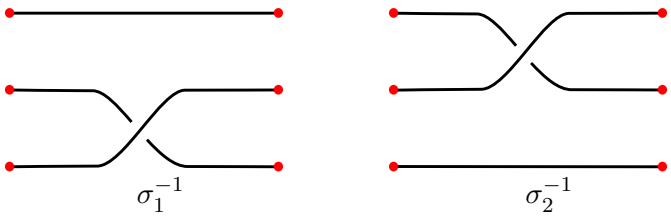

Figure 3.11: The inverses of Artin generators of B_3.

Then, any element in B_n can be realized by concatenating Artin generators and their inverses. For example, the word $\sigma_1\sigma_2\sigma_1\sigma_2^{-1} \in B_3$ is represented by the 3-braid

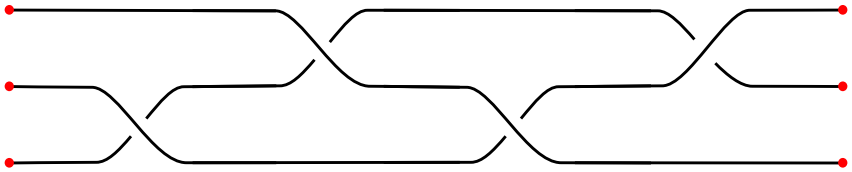

Figure 3.12: 3-braid representing $\sigma_1\sigma_2\sigma_1\sigma_2^{-1} \in B_3$.

Definition 3.3.3. A *band* in B_n is a conjugate of an Artin generator σ_i or an inverse of an Artin generator σ_i^{-1}. In the first case, the band is called *positive* and in the second case, it is called *negative*.

Definition 3.3.4. A *band representation* of a word $\beta \in B_n$ is an ordered set $b = (b_1, \ldots, b_k)$ of bands such that $\beta = \prod_{i=1}^{k} b_i$.

As explained in [24], a band representation b of $\beta \in B_n$ induces a ribbon surface in S^3 bounding the closure of β. This surface is called the *braided surface* associated to b and can be thought of as embedded in $D^2 \times D^2$ with boundary in $\partial D^2 \times D^2$. The figures below depict examples of such surfaces.

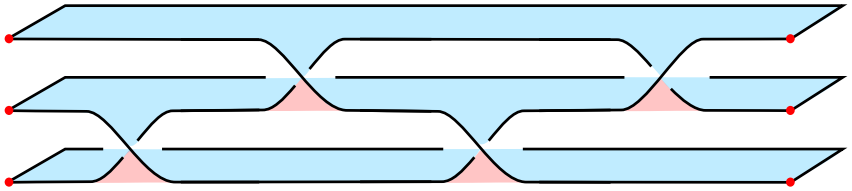

Figure 3.13: Braided surface associated to the band representation $(\sigma_1, \sigma_2, \sigma_1, \sigma_2^{-1})$.

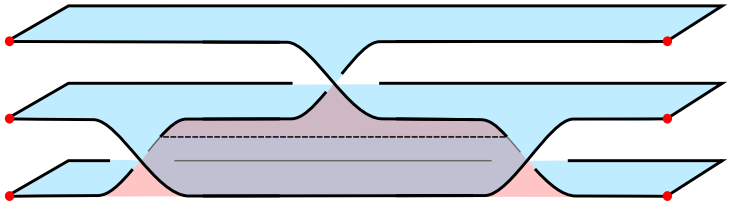

Figure 3.14: Braided surface associated to the band representation $(\sigma_1\sigma_2\sigma_1^{-1})$

Definition 3.3.5. A band representation $b = (b_1, \ldots, b_k)$ is called *quasipositive* if each band b_i is positive.

It turns out that a braided surface arising from a quasipositive band representation always satisfies the following definition.

Definition 3.3.6. A smooth, properly embedded surface F in $\mathbb{D} = \{(z,w) \in \mathbb{C}^2 : |z| \leq 1, |w| \leq 1\}$ is *positively braided* if

(a) ∂F is a braid in $\partial D^2 \times \mathring{D}^2$,

(b) the projection $\pi_{z|F} : F \to D^2$ is a branched covering, and

(c) F is oriented so that $\pi_{z|F}$ is orientation-preserving at all regular points and $\pi_{w|F}$ is orientation-preserving at all branch points (with $D^2 \subset \mathbb{C}$ having the complex orientation).

The following theorem is the ultimate reason why these definitions matter to us.

Theorem 3.3.7 ([23])**.** *A positively braided surface is smoothly isotopic through positively braided surfaces to the intersection of a smooth complex algebraic curve $V \subset \mathbb{C}^2$ with $\mathbb{D}$.*

Hence, our goal now is to realize the surfaces of last section as positively braided surfaces. We will sketch the argument (the full computations and proofs are exhaustively done in [17]).

As a first step, we realize the knot $K = \partial D = \partial D'$ as the closure of a quasipositive braid.

Lemma 3.3.8 ([17], 4.5)**.** *The knot K is smoothly isotopic to the closure of the braid*

$$\beta = (\sigma_2\sigma_3\sigma_2^{-1})(\sigma_1^{-2}\sigma_2\sigma_3\sigma_4^2\sigma_3^{-1}\sigma_2\sigma_3\sigma_4^{-2}\sigma_3^{-1}\sigma_2^{-1}\sigma_1^2)(\sigma_3^{-1}\sigma_2\sigma_1\sigma_2^{-1}\sigma_3)(\sigma_4^{-1}\sigma_3\sigma_4)$$

Furthermore, the bands b, b' and c below get isotoped as shown.

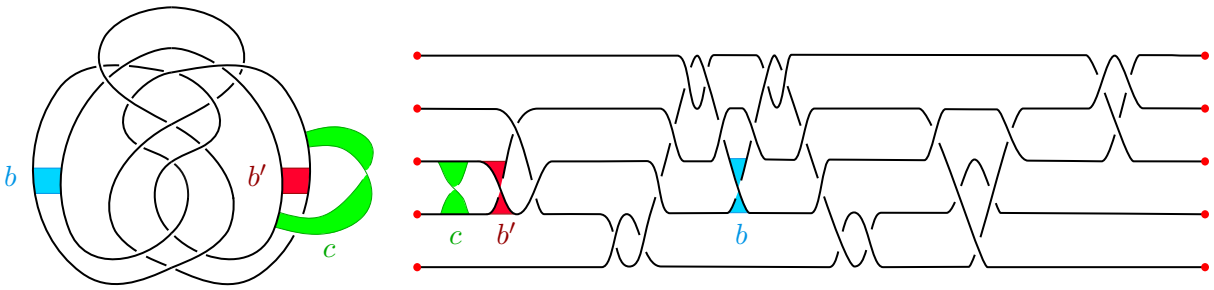

Figure 3.15: The knot K, the braid β and the bands b, b', c.

Notice that the disks D and D' are determined by the band moves b and b', respectively. In order to identify these disks as the positively braided surfaces of some band representation, we will need the following lemma.

Lemma 3.3.9 ([17], 4.3)**.** *Any two positively braided surfaces bounded by the unlink are smoothly isotopic relative boundary.*

Lemma 3.3.10 ([17], 4.4)**.** *The disks D and D' of Figure 3.1 are smoothly isotopic to the positively braided surfaces arising from the band representations of β:*

$$d = (\sigma_2\sigma_3\sigma_2^{-1}, \sigma_1^{-2}\sigma_2\sigma_3\sigma_4^2\sigma_3^{-1}\sigma_2\sigma_3\sigma_4^{-2}\sigma_3^{-1}\sigma_2^{-1}\sigma_1^2, \sigma_3^{-1}\sigma_2\sigma_1\sigma_2^{-1}\sigma_3, \sigma_4^{-1}\sigma_3\sigma_4),$$
$$d' = (\sigma_2, w\sigma_2^{-1}\sigma_1\sigma_2 w^{-1}, w\sigma_2^{-1}\sigma_3\sigma_1\sigma_2\sigma_1^{-1}\sigma_3^{-1}\sigma_2 w^{-1}, w\sigma_3^2\sigma_4\sigma_3^{-2}w^{-1}),$$

where $w = \sigma_3\sigma_4^{-1}\sigma_1^{-1}\sigma_3^{-2}\sigma_2^{-1}\sigma_1^{-1}\sigma_3^{-1}$.

Proof. (sketch) We start with the disk D. By Lemma 3.3.8, it suffices to show that the disk determined by the band move b on the right of Figure 3.15 is smoothly isotopic relative boundary to the disk arising from the band representation d. The former disk is obtained by performing the band move b, which yields an unlink U^2, taking the standard Seifert surface for this unlink and reattaching the band b. On the other hand, the latter disk arises as the braided surface associated to d. Notice that by by removing band b, we get a positively braided surface which also bounds the same unlink U^2. Since standard Seifert surfaces for unlinks are positively braided (after pushing the interiors into the interior of the bidisk $\mathbb{D}$), we can use Lemma 3.3.9 to conclude that these two surfaces bounding the unlink are smoothly isotopic relative boundary. Finally, reattaching the band b yields smoothly isotopic disks, as wanted.

On the other hand, the disk D' is determined by the band move b', which unfortunately does not get isotoped to an Artin generator we are conjugating in the band representation d. In order to fix this, we rewrite ([17], A.1)

$$(\sigma_3\sigma_2^{-1})(\sigma_1^{-2}\sigma_2\sigma_3\sigma_4^2\sigma_3^{-1}\sigma_2\sigma_3\sigma_4^{-2}\sigma_3^{-1}\sigma_2^{-1}\sigma_1^2)(\sigma_3^{-1}\sigma_2\sigma_1\sigma_2^{-1}\sigma_3)(\sigma_4^{-1}\sigma_3\sigma_4)$$

as the quasipositive word

$$(w\sigma_2^{-1}\sigma_1\sigma_2w^{-1})(w\sigma_2^{-1}\sigma_3\sigma_1\sigma_2\sigma_1^{-1}\sigma_3^{-1}\sigma_2w^{-1})(w\sigma_3^2\sigma_4\sigma_3^{-2}w^{-1}).$$

Hence, we obtain a quasipositive band representation d' so that the band b' is realized as the first band in d'. Now, the same argument as above allows us to conclude that D' is smoothly isotopic to the positively braided surface arising from d'. □

Remark 3.3.11. Of course, since the two disks D and D' are smoothly isotopic (under the obvious 180^o rotation), the first part of the proof suffices. However, for the argument that follows, we actually need to realize D' as such braided surface, as we will want to attach bands in a controlled manner to obtain the larger surfaces A', T'. In particular, since in the proof above we have only changed the band representation on the right of the band b', the band c yielding A' will still be attached at the leftmost part of the braided surface as in Figure 3.15.

As a further step towards the proof of Theorem 3.3.1, we now realize the elemental surfaces of the previous section as positively braided surfaces.

Lemma 3.3.12. *The surfaces A, A', T, T', A_0 and T_0 are positively braided surfaces.*

Proof. By Lemma 3.3.8, A and A' smoothly isotopic to the positively braided surfaces arising from the band representations d and d', respectively, after attaching a positive band $\sigma_2 = c$ as in Figure 3.15. Hence, they are positively braided surfaces.

The tori T and T' are obtained by attaching a positive twisted band as in Figure 3.16(a). We isotope this band so that it is braided, at the expense of creating an extra strand as in Figure 3.16(b) below. Notice that all bands are positive, so T and T' are positively braided surfaces.

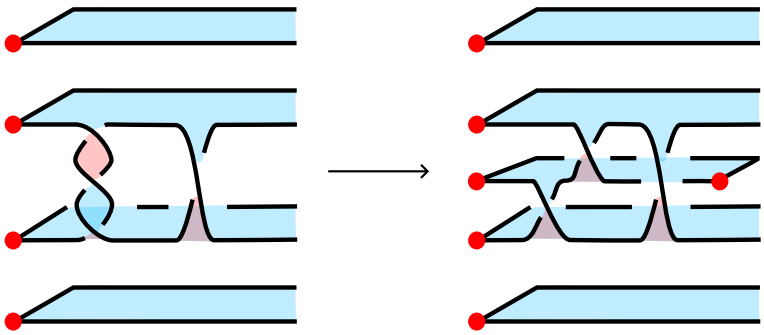

(a) (b)

Figure 3.16: The left portion of the positively braided surfaces realizing the tori T, T'.

For the annulus A_0, simply notice that we can realize it as in Figure 3.17(a) and then perform the same trick.

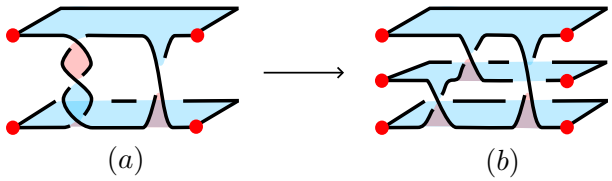

Figure 3.17: The annulus A_0 as a positively braided surface.

Similarly, the torus T_0 is realized in Figure 3.18(a), which again can be transformed into a positively braided surface.

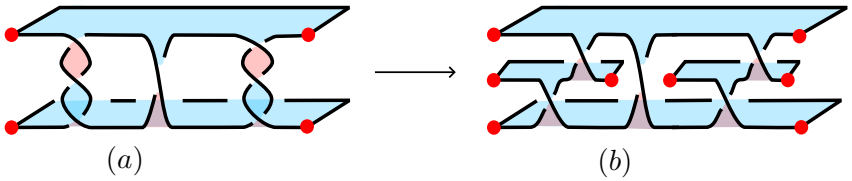

Figure 3.18: The torus T_0 as a positively braided surface.

□

We are now ready to prove the main theorem of this section.

Proof. (of Theorem 3.3.1) Notice that we can boundary connect sum two positively braided surfaces to obtain a positively braided surface: just stack them vertically and attach a positively half-twisted band between them. Hence, since all elemental surfaces A, A', T, T', A_0 and T_0 are positively braided, the surfaces F and F' from Theorem C of the desired topological type $\mathcal{F}$ are also positively braided surfaces. By Theorem 3.3.7, these are smoothly isotopic to compact pieces of algebraic curves $F_0 = V_0 \cap \mathbb{D}$ and $F_1 = V_1 \cap \mathbb{D}$, respectively. This already shows (i).

For (ii) and (iii), notice that we can get from F_0 to F_1 through isotopies which either

- are smooth and keep the boundary in $\partial D^2 \times \mathring{D}^2$, or
- come from homeomorphisms that fix the boundary pointwise.

In the first case, the isotopy is already everywhere smooth. In the second case, we can assume that it is smooth near ∂D by taking a collar neighborhood of $\partial \mathbb{D}$ in $\mathbb{D}$. Also, in either case, the boundary stays in $\partial D^2 \times \mathring{D}^2$.

Finally, (iv) and (v) immediately follow from the proof of Theorem C. □

3.4 Finding a Fatou-Bieberbach domain

In this section, we holomorphically re-embed these complex algebraic curves we just found into $\mathbb{C}^2$. We start by giving the overall idea and then get into the details.

Definition 3.4.1. A *Fatou-Bieberbach domain* is a proper open subset $\Omega \subsetneq \mathbb{C}^n$ that is biholomorphically equivalent to $\mathbb{C}^n$.

By the Riemann mapping theorem, Fatou-Bieberbach domains do not exist for $n = 1$. But they do for any $n > 1$. In fact, this is one of the sort of notions that make complex analysis in several variables fundamentally different than in one variable. This observation also suggests that Fatou-Bieberbach domains are generally very wild and hard to construct.

On the other hand, these domains can be used to construct proper holomorphic embeddings into $\mathbb{C}^2$. For example:

Theorem 3.4.2 ([25]). *There exists a proper holomorphic embedding $\mathring{D}^2 \hookrightarrow \mathbb{C}^2$.*

Proof. (idea) Find a Fatou-Bieberbach domain $\Omega \subset \mathbb{C}^2$ that does not contain a neighborhood of 0 and let L be a complex line that cuts Ω. Argue that $L \cap \Omega$ contains a simply-connected component P that is not all of L. By the Riemann mapping theorem, this component is biholomorphically equivalent to $\mathring{D}^2 \subset \mathbb{C}$. Hence, we may compose these embeddings to obtain a proper holomorphic one

$$\mathring{D}^2 \cong P \hookrightarrow L \cap \Omega \hookrightarrow \Omega \cong \mathbb{C}^2.$$

□

We will use a similar idea, although we will need to have careful control on our choice of Fatou-Bieberbach domains, so that both the topological isotopy and the smooth obstruction are preserved. The following result will provide such control.

Theorem 3.4.3 ([11]). *For any $R > 1$, there exists a Fatou-Bieberbach domain $\Omega \subset \mathbb{C}^2$ such that:*

(i) $\Omega \subseteq \{(z, w) \in \mathbb{C}^2 : |z| < \max(R, |w|)\}$,

(ii) $\Omega \cap (\mathring{D}^2_R \times \mathring{D}^2_R)$ *is an arbitrarily small C^1-perturbation of $\mathring{D}^2_1 \times \mathring{D}^2_R$, and*

(iii) $\partial\Omega := \bar{\Omega} \smallsetminus \Omega$ *is C^1-differentiable and intersects $\mathring{D}^2_R \times \mathring{D}^2_R$ in a C^1-small perturbation of $\partial D^2_1 \times \mathring{D}^2_R$.*

Recall that our goal is to show:

Theorem A ([17]). *There are infinitely many pairs of proper holomorphic curves in $\mathbb{C}^2$ that are exotically knotted.*

We organize the proof in a series of smaller assertions that will be taken care of individually. Following Hayden's notation, given two topological subspaces X, Y of the same topological space, we write (X, Y) to denote the pair $(X, X \cap Y)$.

As a first step, we restate the main result of last section in a more adequate way for the argument that follows.

Assertion 1. *Let F_0 and F_1 be the properly embedded surfaces in $\mathbb{D}$ from last section. They satisfy:*

(a) *F_0 and F_1 are properly and holomorphically embedded in $\mathbb{D}$.*

(b) *F_0 and F_1 are isotopic through homeomorphisms of $\mathbb{D}$ that are smooth in a neighborhood of $\partial\mathbb{D}$.*

(c) *The intermediate surfaces F_t have boundary in $\partial D^2_1 \times \mathring{D}^2_1$.*

(d) *$\Sigma_2(\mathbb{D}, F_0)$ contains a smoothly embedded 2-sphere of square -2.*

(e) *$\Sigma_2(\mathbb{D}, F_1)$ does not contain a smoothly embedded 2-sphere of square -2.*

For $\delta > -1$, define $\mathbb{D}_\delta := D^2_{1+\delta} \times D^2_{1+\delta}$. For convenience, we rescale every pair $(\mathbb{D}, F_t)$ to $(\mathbb{D}_{+\varepsilon}, F_t)$ so that properties $(a) - (e)$ above still hold when replacing $\mathbb{D}$ by $\mathbb{D}_{+\varepsilon}$. Hence, from now on we write $(\mathbb{D}_{+\varepsilon}, F_t)$ for these new rescaled pairs and, as described above, $(\mathbb{D}, F_t)$ will now denote the pair $(\mathbb{D}, \mathbb{D} \cap F_t)$.

Assertion 2. *We may choose $\varepsilon > 0$ so that the three pairs $(\mathbb{D}_{+\varepsilon}, F_i), (\mathbb{D}, F_i), (\mathbb{D}_{-\varepsilon}, F_i)$ are diffeomorphic for $i = 0, 1$.*

Proof. This follows simply by taking adequate collar neighborhoods and use them to define the diffeomorphisms. □

The following assertion claims existence of the Fatou-Bieberbach domain we are interested in.

Assertion 3. *There is a Fatou-Bieberbach domain $\Omega \subset \mathbb{C}^2$ such that*

(1) $\mathbb{D}_{-\varepsilon} \subset \Omega \subset W := \{(z, w) \in \mathbb{C}^2 : |z| < \max(1 + \varepsilon, |w|)$,

(2) each $F_t \cap \Omega$ has the same topological type as $F_t \cap \mathring{\mathbb{D}}^2$,

(3) each $F_t \cap \bar{\Omega}$ is properly embedded in $M := \bar{\Omega} \cap \mathbb{D}_{+\varepsilon}$, and

(4) the isotopy they define is topologically locally flat.

Proof. Fix $R \in (1, 1 + \varepsilon)$ and use Theorem 3.4.3 to get a Fatou-Bieberbach domain $\Omega \subset \mathbb{C}^2$ satisfying properties $(i) - (iii)$. Condition (1) of the assertion is then an immediate consequence of (ii) (for the first inclusion) and of (i) (for the second inclusion).

By (ii), we can choose a Ω as a small enough C^1-perturbation of $\mathring{D}^2_1 \times \mathring{D}^2_R$ so that (2) is satisfied.

By (ii) and (iii), $M = \bar{\Omega} \cap \mathbb{D}_{+\varepsilon}$ is a C^1-manifold. By (iii), $T := \partial\Omega \cap (\mathring{D}^2_R \times \mathring{D}^2_R)$ is an arbitrarily small C^1-perturbation of $\partial D^2_1 \times \mathring{D}^2_R$. If we choose this perturbation small enough, we may assume $T \subset \mathring{\mathbb{D}}_{+\varepsilon} \setminus \mathbb{D}_{-\varepsilon}$. Now, by Assertion $1(b)$, the intermediate surfaces F_t are smooth near $|z| = 1$ and by (c), they are transverse to $\partial D^2_1 \times D^2_R$. By possibly choosing an even smaller C^1-perturbation, we can arrange for F_t to be transverse to T. Hence, $F_t \cap \bar{\Omega}$ will be properly embedded in M. Since t ranges over the compact interval $[0, 1]$, we can choose a fixed Fatou-Bieberbach domain Ω satisfying properties $(1) - (3)$ for every $t \in [0, 1]$.

Finally, since F_0 is smoothly embedded in $\mathbb{D}_{+\varepsilon}$ and the other surfaces F_t are obtained as images of F_0 under homeomorphisms of $\mathbb{D}_{+\varepsilon}$, they are locally flat in $\mathbb{D}_{+\varepsilon}$ and hence also in M. □

Assertion 4. *The isotopy of proper embeddings $F_t \cap \Omega \hookrightarrow \Omega$ is covered by an ambient isotopy of homeomorphisms of Ω.*

In order to prove this we will need an isotopy extension theorem and a lemma:

Theorem ([6], Corollary 1.4)**.** *Let $h_t : N \to M, t \in [0, 1]$, be a locally flat proper isotopy of a compact (topological) manifold N into a (topological) manifold M. Then, h_t is covered by an ambient isotopy of homeomorphisms of M.*

Lemma ([6], Corollary 1.3)**.** *Let $H_t : M \to M, t \in [0, 1]$, be an isotopy of a compact manifold M and let $\{B_i | 1 \leq i \leq p\}$ be an open cover of M. Then, H_t can be written as a composition of isotopies $H_t = H_{k,t} H_{k-1,t} \cdots H_{1,t} H_0$, where each isotopy $H_{j,t} : M \to M$ is an ambient isotopy which is supported by some member of $\{B_i\}$, i.e. $H_{j,t}$ is the identity on the complement of some B_i.*

Proof. (of Assertion 4) Each embedding $F_t \cap \Omega \hookrightarrow \Omega$ is proper because of Assertion 3(3). On the other hand, by the theorem above, $F_t \cap \bar{\Omega} \hookrightarrow M$ is covered by an ambient isotopy of homeomorphisms of M. Since $F_t \subset \mathbb{C} \times \mathring{D}^2_R$, the lemma above allows us to assume that this ambient isotopy fixes every point with $|w| \geq R$. Hence, we can extend the isotopy of homeomorphisms of M by the identity to all of $\bar{\Omega}$. Notice that this isotopy will map the interior of Ω to itself, as it maps the interior of M to itself (because M is a topological manifold) and is the identity elsewhere. Hence, by restricting to the interior, we obtain an ambient isotopy of homeomorphisms of Ω that covers $F_t \cap \Omega \hookrightarrow \Omega$. □

By postcomposing with the biholomorphism $\Omega \cong \mathbb{C}^2$ we can re-embed the surfaces $F_t \cap \Omega$ in $\mathbb{C}^2$. We have:

Assertion 5. *$F_0 \cap \Omega$ and $F_1 \cap \Omega$ are properly and holomorphically embedded in $\mathbb{C}^2$ and are isotopic through homeomorphisms of $\mathbb{C}^2$.*

Proof. The embeddings are proper by Assertion 3(3). They are holomorphic by Assertion 1(a). They are isotopic through homeomorphisms of $\mathbb{C}^2$ by Assertion 4 after pre- and postcomposing by the biholomorphism $\Omega \cong \mathbb{C}^2$. □

It only remains to show that $F_0 \cap \Omega, F_1 \cap \Omega \hookrightarrow \mathbb{C}^2$ are not isotopic through diffeomorphisms of $\mathbb{C}^2$. This will immediately follow from Assertions 7, 8 below. However, we first prove that it makes sense to talk about *the* double branched cover of Ω along $F_i \cap \Omega$. To ease notation, we will denote $F_i \cap \Omega$ simply by F_i.

Assertion 6. *There is a unique (up to diffeomorphism) double branched cover of Ω along F_i.*

Proof. This is essentially the same argument as in the proof of Proposition 1.3.6. By Proposition 1.3.4, it suffices to check that $H_1(\Omega \smallsetminus F_i) \cong \mathbb{Z}$. Consider the Mayer-Vietoris sequence associated to the decomposition $\Omega = (\Omega \smallsetminus F_i) \cup \nu F_i$:

$$\begin{array}{ccccccccc} H_2(\Omega) & \longrightarrow & H_1(\nu F_i \smallsetminus F_i) & \longrightarrow & H_1(\Omega \smallsetminus F_i) \oplus H_1(\nu F_i) & \longrightarrow & H_1(\Omega) \\ \| & & \wr\| & & \wr\| & & \| \\ 0 & \longrightarrow & H_1(S^1) \oplus H_1(F_i) & \longrightarrow & H_1(\Omega \smallsetminus F_i) \oplus H_1(F_i) & \longrightarrow & 0 \end{array}$$

Under our identifications, the $H_1(F_i)$ summand on the left gets mapped to the $H_1(F)$ summand on the right, so $H_1(\Omega \smallsetminus F_i) \cong H_1(S^1) \cong \mathbb{Z}$. □

Assertion 7. *$\Sigma_2(\Omega, F_0)$ contains a smoothly embedded 2-sphere of square -2.*

Proof. By Assertion 3(1), $\mathring{\mathbb{D}}_{-\varepsilon}$ is contained in Ω. Hence, the double branched cover $\Sigma_2(\mathring{\mathbb{D}}_{-\varepsilon}, F_0)$ smoothly embeds in $\Sigma_2(\Omega, F_0)$. By Assertion 2, we have a diffeomorphism $\Sigma_2(\mathbb{D}_{-\varepsilon}, F_0) \cong \Sigma_2(\mathbb{D}_{+\varepsilon}, F_0)$. Hence, also $\Sigma_2(\mathring{\mathbb{D}}_{+\varepsilon}, F_0)$ smoothly embeds in $\Sigma_2(\Omega, F_0)$. By Assertion 1(d), $\Sigma_2(\mathring{\mathbb{D}}_{+\varepsilon}, F_0)$ contains a smoothly embedded 2-sphere of square -2 and hence so does $\Sigma_2(\Omega, F_0)$. □

Assertion 8. *$\Sigma_2(\Omega, F_1)$ does not contain a smoothly embedded 2-sphere of square -2.*

Proof. By Assertion 3(1), Ω is contained in W. Hence, the double branched cover $\Sigma_2(\Omega, F_1)$ smoothly embeds in $\Sigma_2(W, F_1)$. Via radial scale, there is a diffeomorphism $(W, F_1) \cong (\mathring{\mathbb{D}}_{+\varepsilon}, F_1)$, so $\Sigma_2(\Omega, F_1)$ smoothly embeds in $\Sigma_2(\mathbb{D}_{+\varepsilon}, F_1)$. If $\Sigma_2(\Omega, F_1)$ contained a smoothly embedded 2-sphere of square -2, then so would $\Sigma_2(\mathbb{D}_{+\varepsilon}, F_1)$, contradicting Assertion 1(e). □

Chapter 4

Extending the construction

The goal of this chapter is to present some extensions of the construction given above.

In Section 4.1, we construct arbitrarily large tuples of pairwise exotically knotted surfaces in B^4 relative boundary. We do this for both the orientable and non-orientable case. That is, we prove Theorem D.

In Section 4.2, we extend Theorem C to the non-orientable case, i.e. construct pairs of exotically knotted non-orientable surfaces in B^4 whose interiors remain exotically knotted. That is, we prove Theorem E.

In Section 4.3, we first construct some tuples of exotically knotted surfaces in B^4 whose interiors remain exotically knotted. That is, we prove Theorem F.

4.1 Tuples of exotically knotted surfaces relative boundary

As mentioned above, the goal of this section is to prove:

Theorem D. *Let $n \in \mathbb{N}$. Any compact, connected surface with boundary admits a 2^n-tuple of smooth, proper embeddings in B^4 that are pairwise exotically knotted relative boundary.*

This result was proven for the disk in [19] by distinguishing cobordism maps on Khovanov homology In fact, even though we use a different obstruction, the construction we present is the same one.

Let us do this first for the disk and $n = 3$ and then prove the general case (which will be essentially the same argument). The idea is to take boundary connected sums of three copies of either D or D' by forming sorts of windmills (see Figure 4.1 below). Since we are taking three copies of the disks, there will be $2^3 = 8$ possible ways to boundary connect sum them. Notice also that the 8 resulting disks will be topologically isotopic relative boundary, as the disks D and D' were. We claim that these 8 disks are pairwise not smoothly isotopic relative boundary. We argue by contradiction. Suppose that a pair of them is smoothly isotopic relative boundary. This pair will then differ in some boundary connected summand, i.e. one will have a D where the other has a D'. For the sake of clarity, let us say the pair is as in Figure 4.1.

Since we are assuming that this pair is smoothly isotopic relative boundary, we can attach a band in the same way to both surfaces and the result will still be smoothly isotopic relative boundary. We choose to attach a band as in the previous chapter. Namely, we obtain the annuli of Figure 4.2.

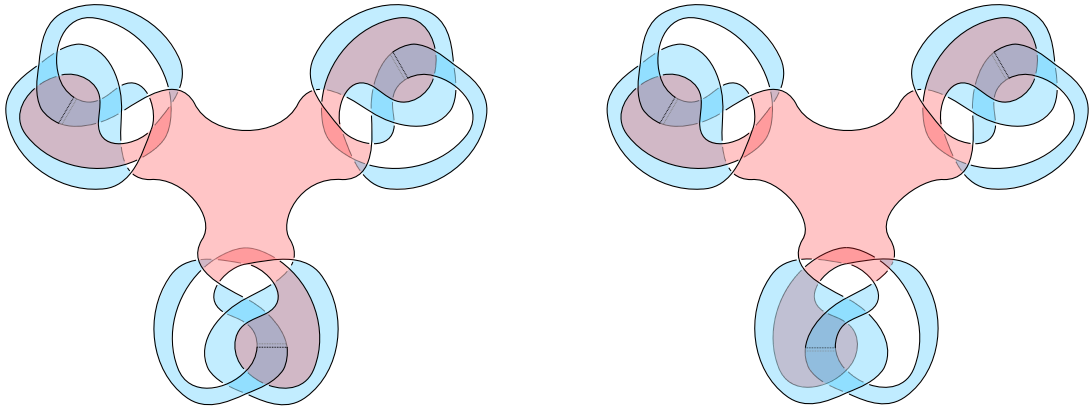

Figure 4.1: A pair of exotically knotted disks in B^4 relative boundary.

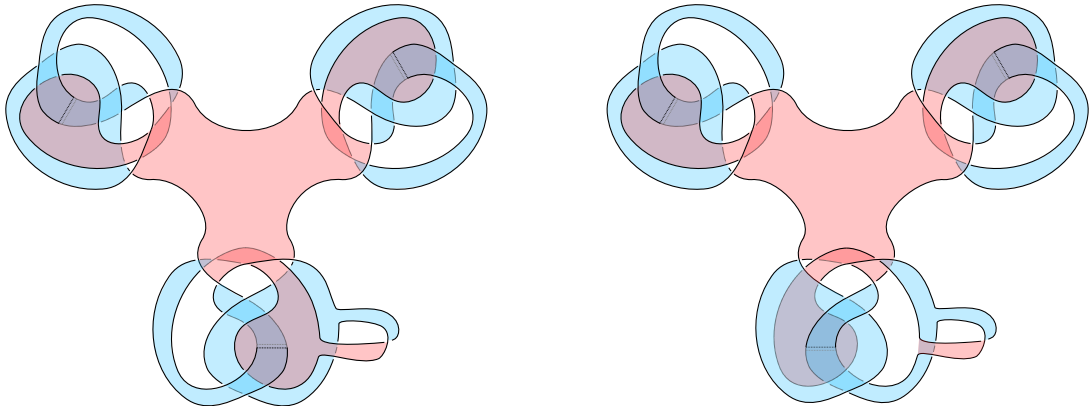

Figure 4.2: A pair of exotically knotted annuli in B^4.

Notice that the double branched cover along the annulus on the right contains the leftmost Kirby diagram of Lemma A.3 in the appendix. Arguing as in the proof of Proposition 3.2.1, we conclude that this double branched cover contains a smoothly embedded 2-sphere of square -2.

However, the double branched cover along the annulus on the left decomposes as the sum $W = \Sigma_2(B^4, D) \natural \Sigma_2(B^4, D) \natural \Sigma_2(B^4, A)$ and hence admits a Stein structure with $\langle c_1(W), h_1 \rangle = -2$, where h_1 is the homology class represented by the 2-handle of $\Sigma_2(B^4, A)$. Since $H_2(W) = \langle h_1 \rangle \cong \mathbb{Z}$, a smoothly embedded 2-sphere S with $[S]^2 = -2$ must satisfy $[S] = \pm h_1$ and hence $\langle c_1(W), [S] \rangle = \mp 2$, contradicting Theorem 2.2.7. Thus, the annuli in Figure 4.2 are exotically knotted and the pair of disks in Figure 4.1 are exotically knotted relative boundary.

Notice that the argument for a general $n \in \mathbb{N}$ is no different from this.

In order to extend this to arbitrary compact, connected orientable surfaces with boundary we simply consider the same boundary connected sum of disks and further boundary sum with the necessary copies of the annuli A_0 and torus-with-1-hole T_0 of Figure 3.8. Since the double branched covers along A_0 and T_0 admit Stein structures and have Kirby diagrams shown in Figure 3.9, our argument will descend nicely in this case.

Finally, in order to construct the non-orientable tuples, we consider the following Möbius band M_0.

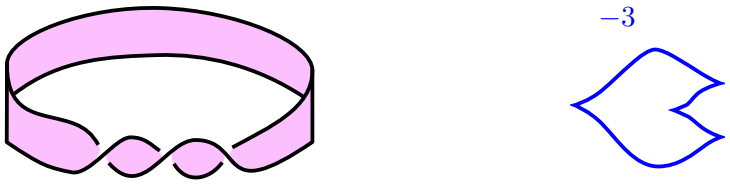

Figure 4.3: The Möbius band M_0 (left) and a Kirby diagram of $\Sigma_2(B^4, M_0)$ in standard form.

Since $\Sigma_2(B^4, M_0)$ also admits a Stein structure and its linking matrix is simply $[-3]$, the previous argument will descend nicely again. This concludes the proof of Theorem D.

4.2 The non-orientable case

The goal of this section is to prove:

Theorem E. *Any compact, connected, non-orientable surface with boundary admits a pair of smooth, proper embeddings in B^4 that are exotically knotted. Furthermore, they remain exotically knotted when restricted to the interior.*

The idea will be the same as in Section 3.2. Let us consider the Möbius bands M and M' of Figure 4.4 below. Notice that even though red and blue colors do not represent a side of the surface anymore, we keep them because they help to visualize the surface.

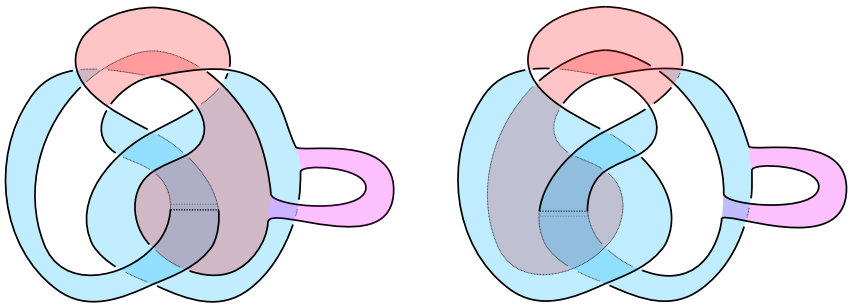

Figure 4.4: The Möbius bands M (left) and M' (right).

As always, notice that M and M' are topologically isotopic relative boundary, because the disks D and D' were.

On the other hand, notice that the double branched cover along M' contains a smoothly embedded 2-sphere of square -1. Indeed, M' contains the Möbius band F_{-1} of Figure 1.13. By the computation below that figure, $\Sigma_2(B^4, F_{-1})$ contains such a sphere and hence also does $\Sigma_2(B^4, M')$. In particular, Theorem 2.2.7 implies that $\Sigma_2(B^4, M')$ does not admit a Stein structure. Hence, the following lemma (which is proven in the appendix) suffices to obstruct a smooth isotopy between M and M'.

Lemma A.4. *The double branched cover $\Sigma_2(B^4, M)$ has Kirby diagram:*

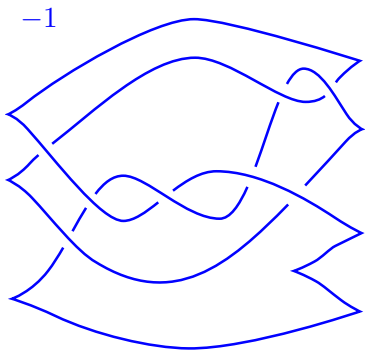

Figure 4.5: Kirby diagram for $\Sigma_2(B^4, M)$.

The shown attaching sphere has $tb = 0$ and hence $\Sigma_2(B^4, M)$ admits a Stein structure.

Now, to obtain pairs of compact, connected non-orientable exotically knotted surfaces of any topological type, we simply boundary connect sum M and M' with the simpler annulus A_0 and Möbius band M_0. The resulting surfaces will be exotically knotted by the same argument as in Section 3.2. This completes the proof of Theorem E.

4.3 Tuples of exotically knotted surfaces

The goal of this section is to prove the following result:

Theorem F. *Let $g \geq 0, h \geq 1 \in \mathbb{N}$ not both equalities. The compact, connected, orientable surface with boundary with-h-holes and genus g admits a $(g+1)h$-tuple of smooth, proper embeddings in B^4 that are pairwise exotically knotted. Furthermore, they remain exotically knotted when restricted to the interior.*

We first show the weaker version:

Lemma 4.3.1. *Let $g \geq 0, h \geq 1 \in \mathbb{N}$ not both equalities. The compact, connected, orientable surface with boundary with-h-holes and genus g admits a $(g+h)$-tuple of smooth, proper embeddings in B^4 that are pairwise exotically knotted. Furthermore, they remain exotically knotted when restricted to the interior.*

As a first step, we note that even though $\Sigma_2(B^4, A'), \Sigma_2(B^4, T')$ contain a smoothly embedded 2-sphere of square -2, they admit a Stein structures (the proof can be found in the appendix.

Lemma A.3. *The double branched covers $\Sigma_2(B^4, A')$ and $\Sigma_2(B^4, T')$ have Kirby diagrams:*

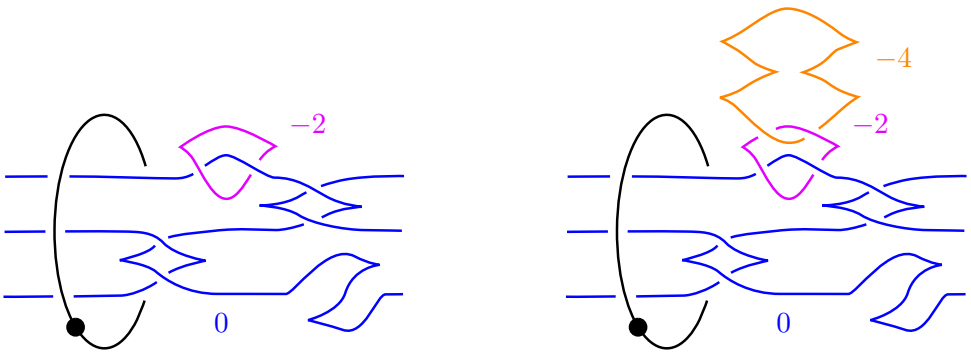

Figure 4.6: Kirby diagrams for $\Sigma_2(B^4, A')$ and $\Sigma_2(B^4, T')$ in standard form.

In particular, they admit Stein structures.

As in Section 4.1, we first prove Lemma 4.3.1 for a particular case and the general proof will be essentially the same. Suppose, for example, that $g = 1$ and $h = 3$. Our goal is then to construct a 4-tuple of pairwise exotically knotted embeddings of the compact, connected surface with boundary with-3-holes and genus 1 in B^4. The trick is very similar to the one in Section 4.1. Consider the surfaces depicted in Figure 4.7 below.

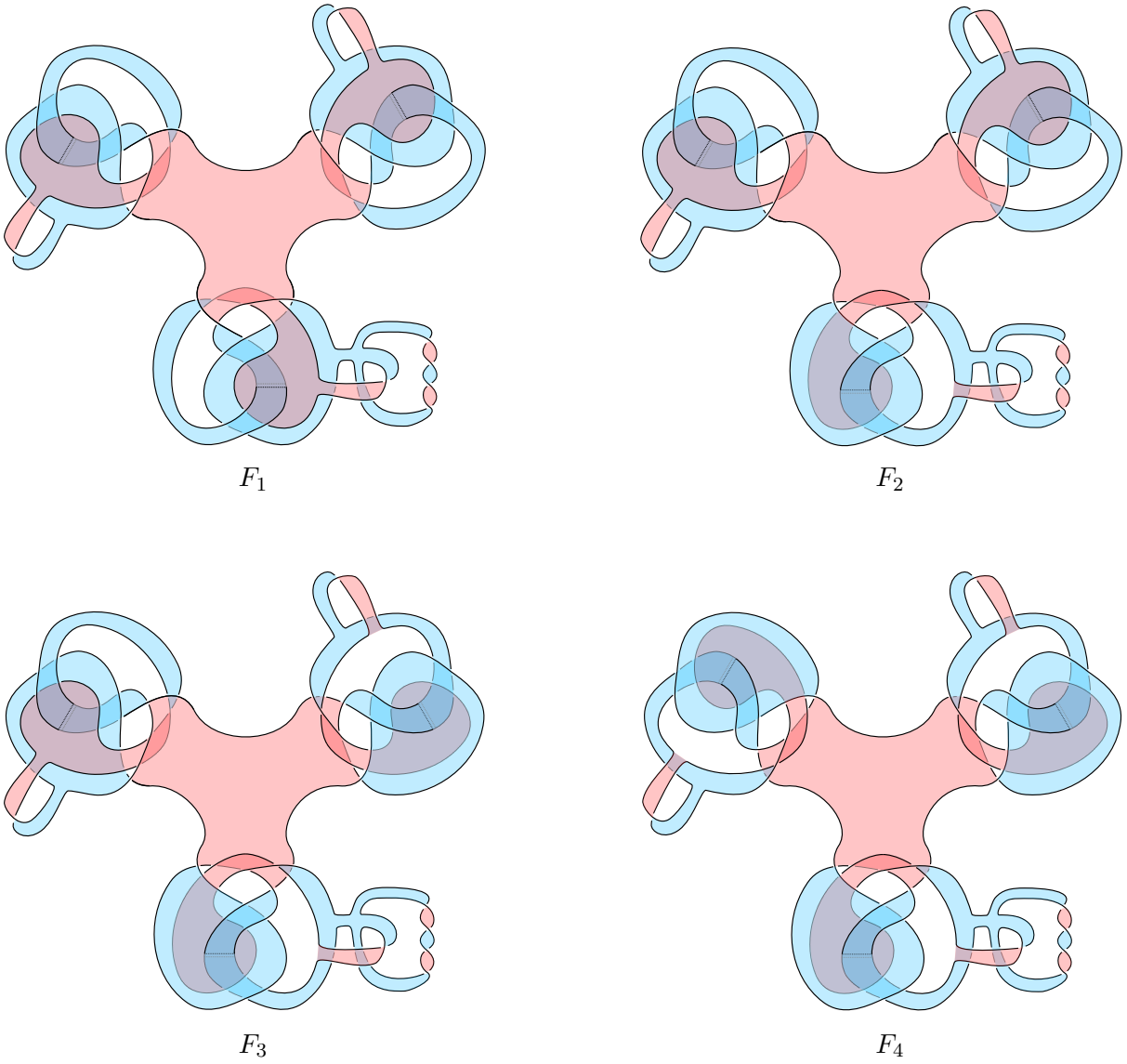

Figure 4.7: Four exotically knotted surfaces with-3-holes and genus 1 in B^4.

Again, these surfaces are topologically isotopic relative boundary, because the disks D and D' were. Furthermore, by Lemma A.3 the double branched covers $\Sigma_2(B^4, F_i)$ admit Stein structures. The following claim will be enough to assert that the surfaces F_i are pairwise not smoothly isotopic (not even restricting to the interiors).

Claim 4.3.2. *$\Sigma_2(B^4, F_i)$ has exactly $i-1$ linearly independent homology classes in $H_2(W)$ that can be represented by a smoothly embedded 2-sphere of square -2.*

Proof. By Lemma A.3 in the appendix, $\Sigma_2(B^4, F_i)$ has at least $i-1$ such homology classes. The fact that there are no more than these follows by the same argument as in Section 3.2 using the obstruction from Theorem 2.2.7. □

The argument for general g and h is the same, one just boundary connect sums with more copies of A, A', T and T'. This finishes the proof of Lemma 4.3.1.

In order to prove the stronger version Theorem F, we just have to note that there are even more homology classes that can be distinguished. Indeed, by Lemmas A.2 and A.3, the homology classes associated to the tori, intersect non-trivially with other homology classes. Hence, we are able not only to count the number of linearly independent homology classes that can be represented by a smoothly embedded 2-sphere of square -2, but also the number of linearly independent homology classes that intersect non-trivially with other classes and the number of those that do not. A simple counting computation shows that there are $(g+1)h$ possibilities that we can distinguish in this way. This proves Theorem F.

To end this section, we explain what is needed to upgrade these surfaces to exotically knotted complex curves as we did through Sections 3.3 and 3.4.

Suppose we have fixed g and h and we have our n-tuple of exotically knotted surfaces $(F_1, \dots, F_n)$, where $n = g + h$ and $\Sigma_2(B^4, F_i)$ has exactly $i - 1$ linearly independent homology classes in $H_2(W)$ that can be represented by a smoothly embedded 2-sphere of square -2.

Since boundary connected sums of braided surfaces can be realized by stacking them vertically and joining them using positive bands, the surfaces $F_1, \dots, F_n$ are positively braided and hence can be thought of as compact pieces of complex algebraic curves in $\mathbb{C}^2$.

Now, we have to adapt the step of finding a suitable Fatou-Bieberbach domain. Until Assertion 5, everything goes through without any major modifications, i.e. we find a Fatou-Bieberbach domain $\Omega \subset \mathbb{C}^2$ such that all $F_i \cap \Omega$ are properly and holomorphically embedded and are isotopic through homeomorphisms of $\mathbb{C}^2$.

In order to obstruct smooth isotopies, we again propose distinguishing the double branched covers $\Sigma_2(\Omega, F_i)$. This time, however, this becomes much harder than when we had only one pair to distinguish, as we need certain control over the homology classes of $\Sigma_2(\Omega, F_i)$. We start by showing:

Lemma 4.3.3. *Let Y^m be a smooth manifold, F^{m-2} a smoothly and properly embedded codimension 2 submanifold and $X^m \subset Y^m$ a submanifold. Suppose also that*

(i) $H_1(Y \smallsetminus F) \cong H_1(X \smallsetminus F) \cong \mathbb{Z}$ (so double covers are unique),

(ii) the inclusion $F \cap X \hookrightarrow F$ is a homotopy equivalence, and

(iii) the inclusion $X \smallsetminus F \hookrightarrow Y \smallsetminus Y$ is also a homotopy equivalence.

Then, the inclusion $\Sigma_2(X, F) \hookrightarrow \Sigma_2(Y, F)$ induces isomorphisms in homology.

Proof. To ease notation, we write $F \cap X$ as simply F (property (ii) ensures that everything still makes sense). Also, let $\tilde{X}$ denote the double cover $\Sigma_2(X, F) \smallsetminus F$ of $X \smallsetminus F$ and, similarly, let $\tilde{Y}$ denote the double cover $\Sigma_2(Y, F) \smallsetminus F$ of $Y \smallsetminus F$. Lifting $\tilde{X} \to X \smallsetminus F \hookrightarrow Y \smallsetminus F$ and using (i) and (iii) gives a homotopy equivalence $\tilde{X} \hookrightarrow \tilde{Y}$. We can now consider the Mayer-Vietoris sequences associated to the decompositions $\Sigma_2(X, F) = \tilde{X} \cup \nu F$ and $\Sigma_2(Y, F) = \tilde{Y} \cup \nu F$ gives a commutative diagram:

$$\begin{array}{ccccccccc}
H_n(\nu F \smallsetminus F) & \to & H_n(\tilde{X}) \oplus H_n(F) & \to & H_n(\Sigma_2(X,F)) & \to & H_{n-1}(\nu F \smallsetminus F) & \to & H_{n-1}(\tilde{X}) \oplus H_{n-1}(F) \\
\downarrow \cong & & \downarrow \cong & & \downarrow & & \downarrow \cong & & \downarrow \cong \\
H_n(\nu F \smallsetminus F) & \to & H_n(\tilde{Y}) \oplus H_n(F) & \to & H_n(\Sigma_2(Y,F)) & \to & H_{n-1}(\nu F \smallsetminus F) & \to & H_{n-1}(\tilde{Y}) \oplus H_{n-1}(F)
\end{array}$$

The 5-Lemma finishes the proof. □

Applying the lemma to the inclusion of pairs $(\mathring{\mathbb{D}}_{-\varepsilon}, F_i) \hookrightarrow (W, F_i)$, we get that the inclusion $\Sigma_2(\mathring{\mathbb{D}}_{-\varepsilon}, F_i) \hookrightarrow \Sigma_2(W, F_i) \cong_{sm} \Sigma_2(\mathring{\mathbb{D}}_{+\varepsilon}, F_i)$ induces isomorphisms in homology. Since it factors through $\Sigma_2(\Omega, F_i)$, the isomorphism $H_2(\Sigma_2(\mathring{\mathbb{D}}_{-\varepsilon}, F_i)) \xrightarrow{\cong} H_2(\Sigma_2(\mathring{\mathbb{D}}_{+\varepsilon}, F_i))$ also factors through $H_2(\Omega, F_i)$. Hence, inclusions induce an injective map followed by a surjective map:

$$H_2(\Sigma_2(\mathring{\mathbb{D}}_{-\varepsilon}, F_i)) \hookrightarrow H_2(\Omega, F_i) \twoheadrightarrow H_2(\Sigma_2(\mathring{\mathbb{D}}_{+\varepsilon}, F_i))$$

Since $\Sigma_2(\mathring{\mathbb{D}}_{-\varepsilon}, F_i)$ has $i-1$ linearly independent homology classes in H_2 that can be represented by a smoothly embedded 2-sphere of square -2, so will $\Sigma_2(\Omega, F_i)$.

However, we have no guarantee that $\Sigma_2(\Omega, F_i)$ has no more than $i-1$ such classes, as its second homology could potentially be larger than $H_2(\Sigma_2(\mathring{\mathbb{D}}_{+\varepsilon}, F_i))$. For that, it would suffice that the free part of $H_2(\Sigma_2(\Omega, F_i)$ is $H_2(\Sigma_2(\mathring{\mathbb{D}}_{+\varepsilon}, F_i)) \cong \mathbb{Z}^{2g+h-1}$. In order to achieve this, further control over the choice of the Fatou-Bieberbach domain is needed. For example, by the Lemma above, it suffices if the inclusion $\mathring{\mathbb{D}}_{-\varepsilon} \smallsetminus F_i \hookrightarrow \Omega \smallsetminus F_i$ is a homotopy equivalence. Hence, we have:

Remark 4.3.4. If the Fatou-Bieberbach domain $\Omega \subset \mathbb{C}^2$ above can be chosen so that the inclusions $\mathring{\mathbb{D}}_{-\varepsilon} \smallsetminus F_i \hookrightarrow \Omega \smallsetminus F_i$ are homotopy equivalences, then all $F_i \cap \Omega$ are properly and holomorphically embedded in $\mathbb{C}^2$ and pairwise exotically knotted.

Appendix

Lemma A.1. *A Kirby diagram of the double branched cover $\Sigma_2(B^4, D)$ is shown on the right of Figure 4.8. Furthermore, the loops γ and γ' on the left, have lifts $\tilde{\gamma}$ and $\tilde{\gamma}'$, respectively.*

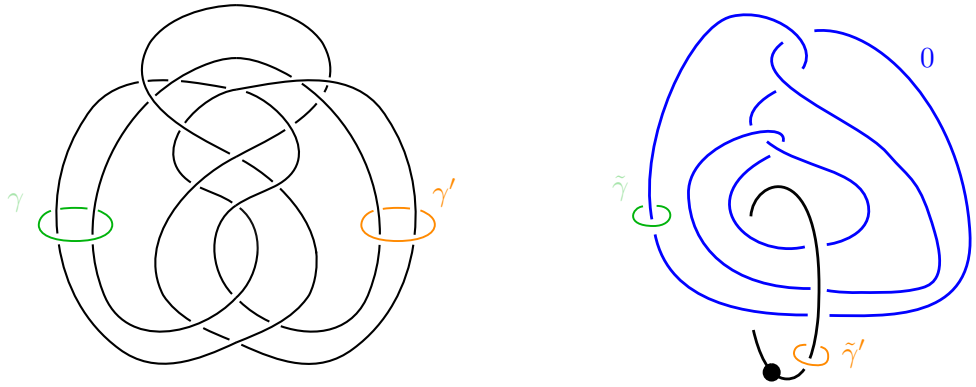

Figure 4.8: The knot K together with two loops γ and γ' (left). The double branched cover $\Sigma_2(B^4, D)$ together with lifts of γ and γ' (right).

Proof. We start by producing a Kirby diagram for $B^4 \setminus \nu D$ and make this diagram look like in Lemma 1.3.8 so that we can use it without complications.

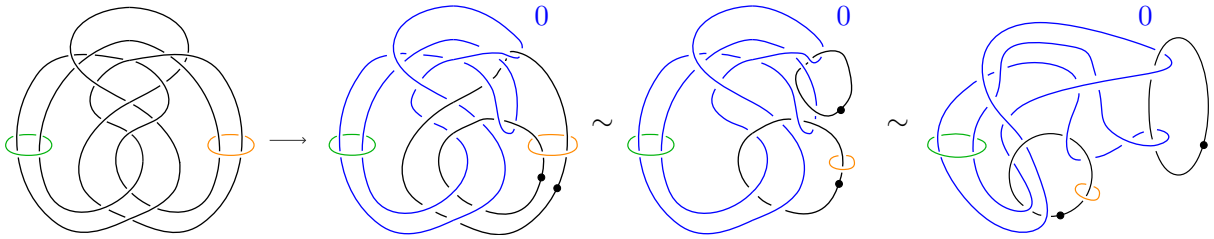

Figure 4.9: The complement $B^4 \setminus \nu D$ together with a pair of loops.

Now, using Lemma 1.3.8, we obtain the Kirby diagram of Figure 4.10. Notice that the framing coefficients of both 2-handles are 0, because of Equation 1.1, where $fr(h_Y) = 0$, $wr(h_X) = 2$ and $wr(h_Y) = 1$.

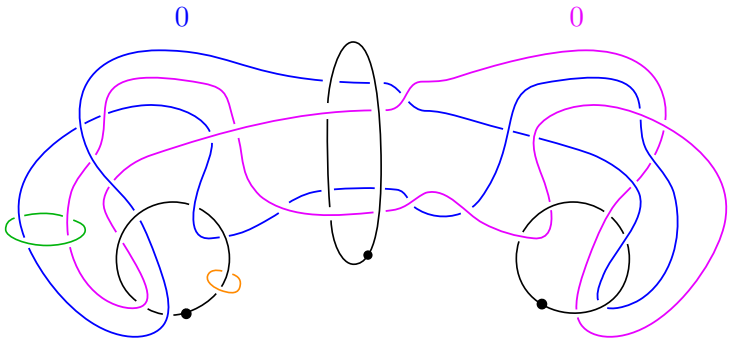

Figure 4.10: The double cover of $B^4 \setminus \nu D$.

Notice also that by attaching a single cancelling 0-framed 2-handle to the rightmost dotted circle of Figure 4.9, we recover B^4. Hence, to the double cover of $B^4 \setminus \nu D$, we just need to remove the lift of this dotted circle to obtain a Kirby diagram of the double branched cover $\Sigma_2(B^4, D)$. This way, we get Figure 4.11.

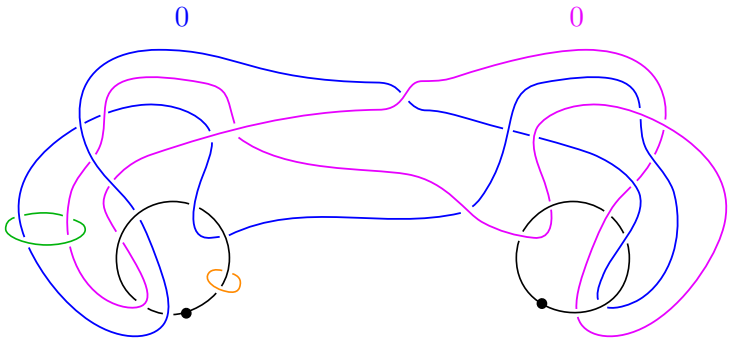

Figure 4.11: The double branched cover $\Sigma_2(B^4, D)$.

The remaining steps will just consist of simplifications of this diagram. As a first step, we obtain Figure 4.12 by sliding the pink 2-handle over the blue one using Proposition 1.2.2.

Next, we want to cancel the rightmost dotted circle with the pink 2-handle. Before doing that, though, we need to slide the blue 2-handle over the pink one so that it does not go through the dotted circle anymore. The result of the handle slide is given in Figure 4.13 and the result after cancelling is pictured in Figure 4.14.

Finally, Figure 4.15 gives the isotopies that lead to the positron cork of the previous chapter.

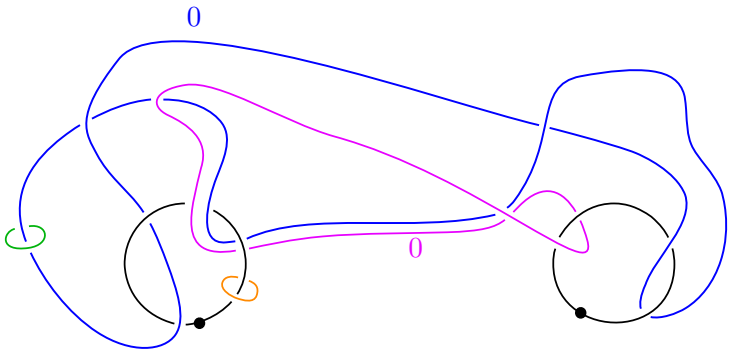

Figure 4.12: The double branched cover $\Sigma_2(B^4, D)$ after one handle slide.

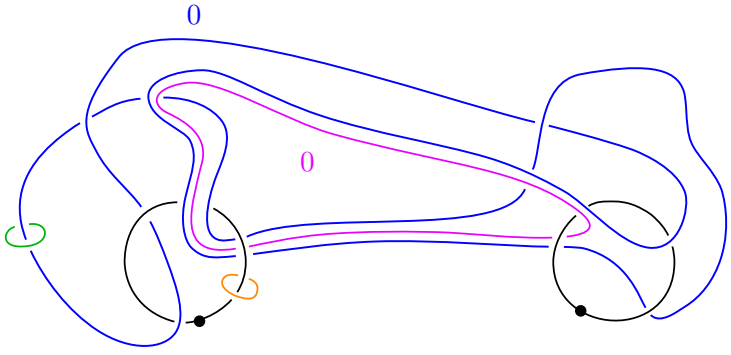

Figure 4.13: The double branched cover $\Sigma_2(B^4, D)$ after a second handle slide.

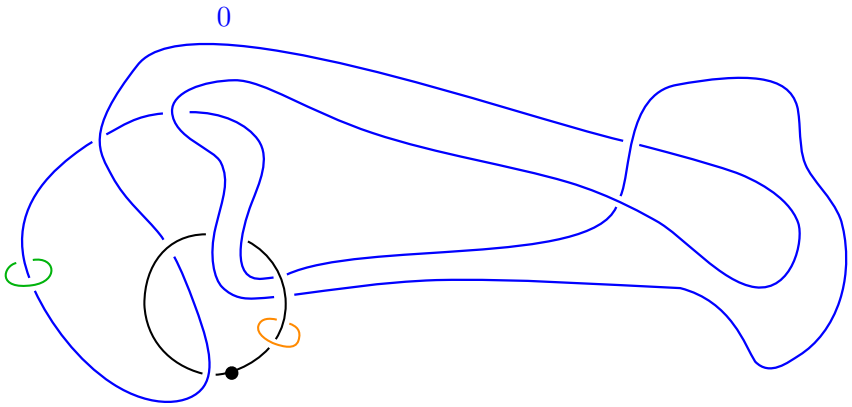

Figure 4.14: The double branched cover $\Sigma_2(B^4, D)$ after cancelling handles.

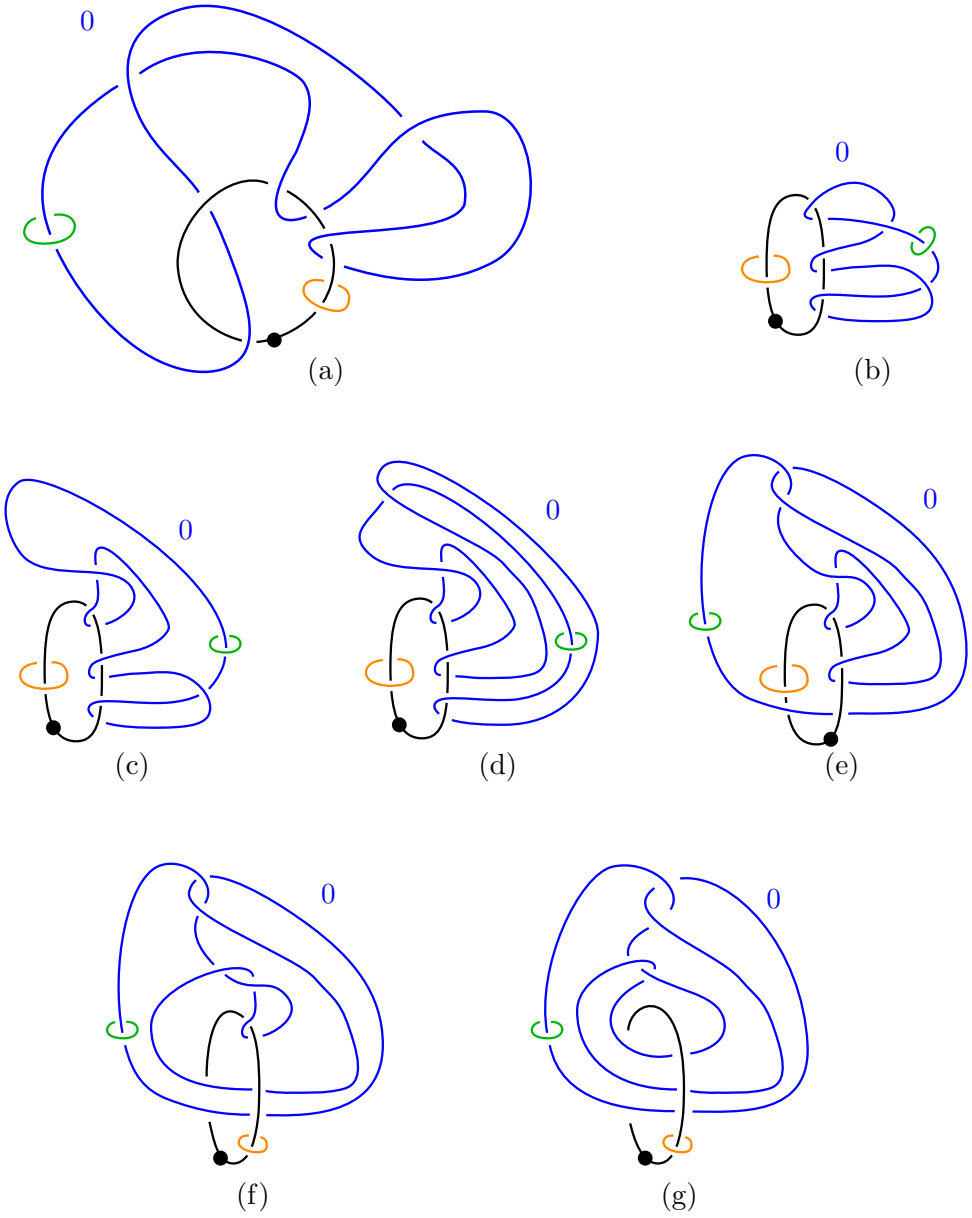

Figure 4.15: Isotopies showing that $\Sigma_2(B^4, D)$ is the positron cork.

□

Lemma A.2. *The following are Kirby diagrams for the double branched covers* $\Sigma_2(B^4, A)$ *and* $\Sigma_2(B^4, T)$*, respectively.*

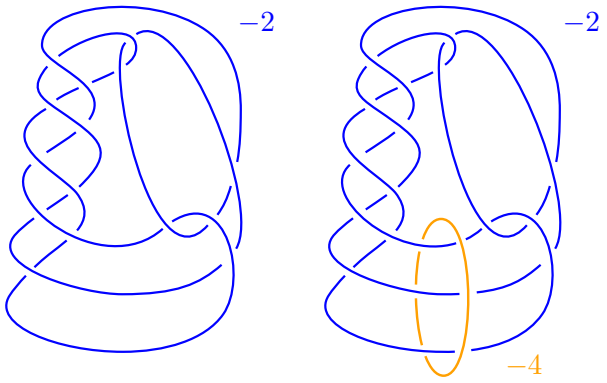

Figure 4.16: Kirby diagrams of $\Sigma_2(B^4, A)$ (left) and $\Sigma_2(B^4, T)$ (right).

Proof. We present the computation of the rightmost diagram. For the other diagram, one just has to ignore the orange 2-handle throughout the proof. As in the previous lemma, we start by producing a Kirby diagram of the complement $B^4 \setminus \nu T$ and making it look like in Lemma 1.3.8. This is done in Figure 4.17.

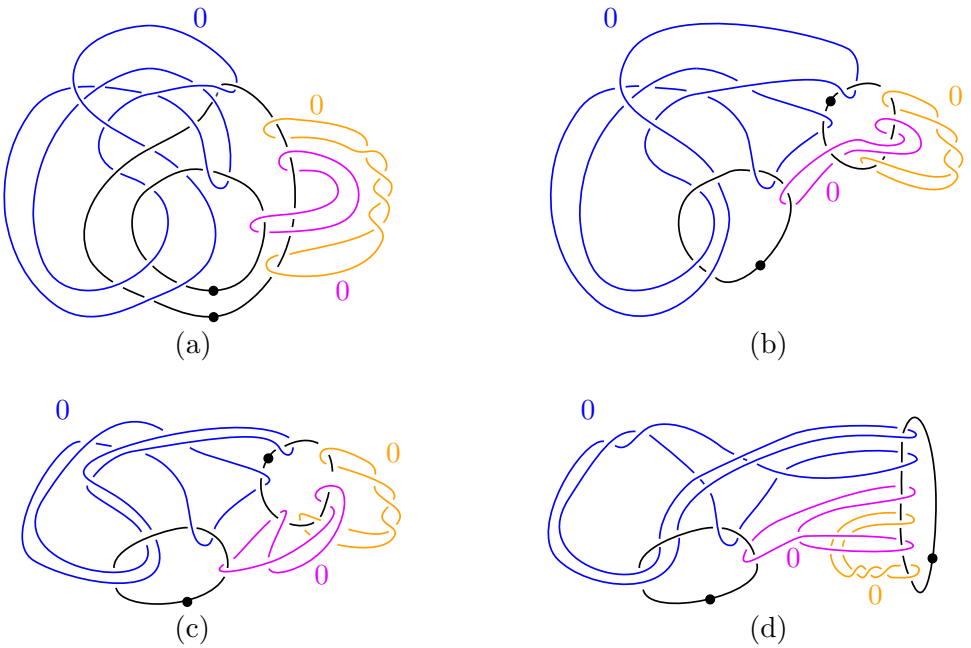

Figure 4.17: Equivalent Kirby diagrams of $B^4 \setminus \nu T$. From (a) to (b), we have performed a 1-handle slide. The other steps are simply isotopies.

Now we can use Lemma 1.3.8 to produce a Kirby diagram of the double cover of $B^4 \setminus \nu T$. Notice that in order to recover B^4 from $B^4 \setminus \nu T$, we need to attach a 2-handle to cancel the rightmost dotted circle and a 3-handle to cancel the blue 2-handle. Hence, we obtain the following Kirby diagram diagram of $\Sigma_2(B^4, T)$ after cancelling the 1-/2-handle pair:

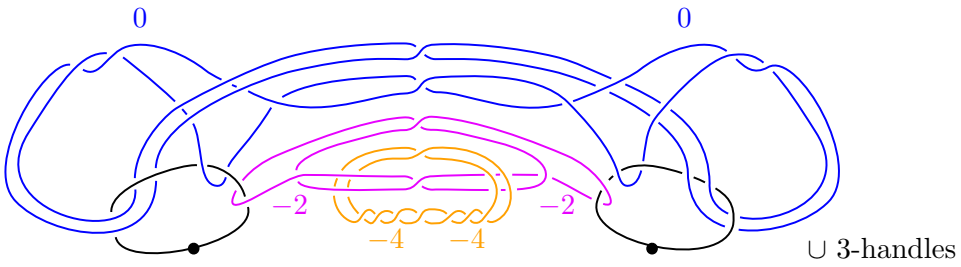

Figure 4.18: Kirby diagram of $\Sigma_2(B^4, T)$ before cancelling the 2-/3-handle pair.

The following steps are simplifications of the diagram above:

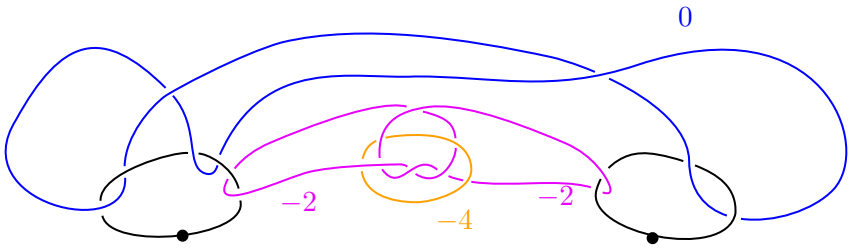

Figure 4.19: Kirby diagram of $\Sigma_2(B^4, T)$ after cancelling the 2-/3-handle pair.

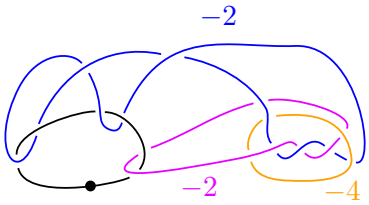

Figure 4.20: Kirby diagrams of $\Sigma_2(B^4, T)$ after sliding the blue 2-handle over the rightmost pink one and cancelling the 1-/2-handle pair.

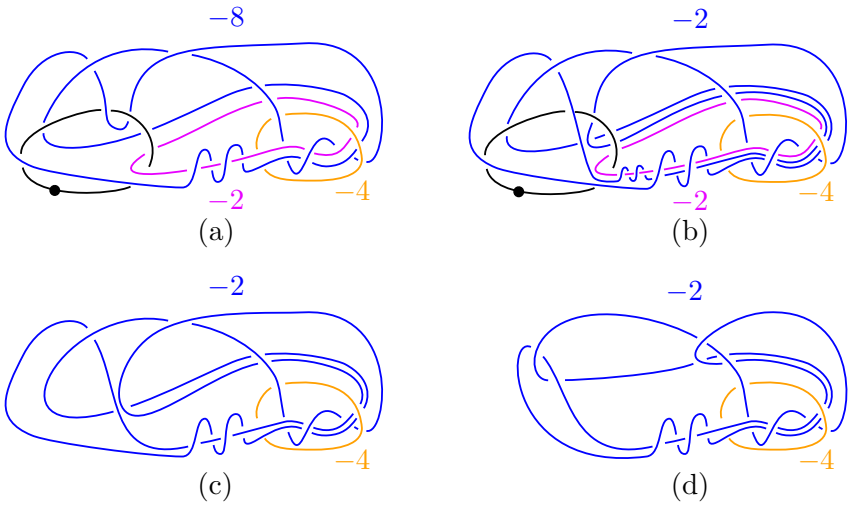

Figure 4.21: Equivalent Kirby diagrams of $\Sigma_2(B^4, T)$. At (a), we have slid the blue 2-handle over the pink one. At (b), we have again done that so that the blue 2-handle does not go through the 1-handle anymore. At (c), we have cancelled the 1-/2-handle pair. The other steps are simply isotopies.

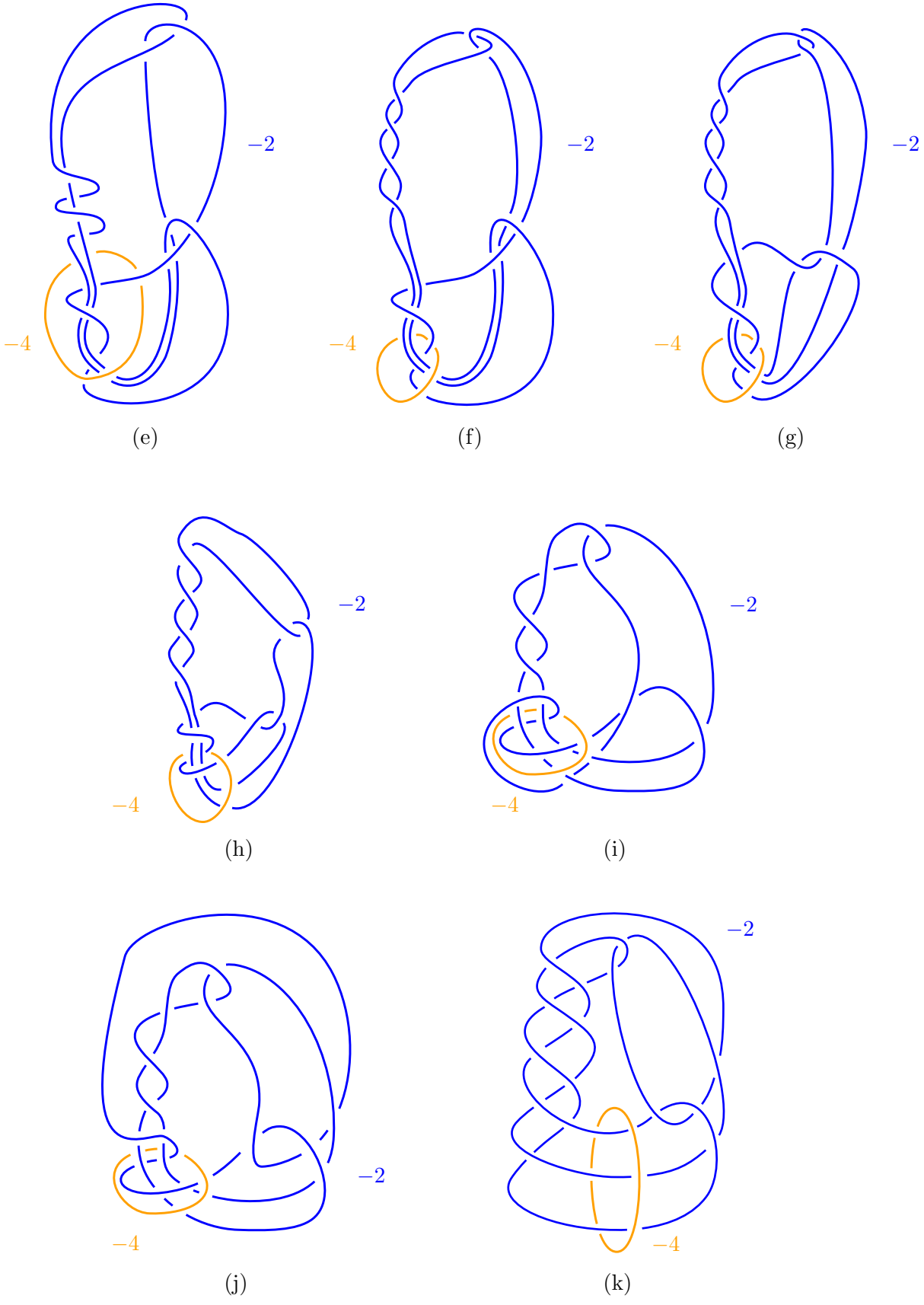

Figure 4.22: Equivalent Kirby diagrams of $\Sigma_2(B^4, T)$ related by isotopies.

□

Lemma A.3. *The double branched covers $\Sigma_2(B^4, A')$ and $\Sigma_2(B^4, T')$ have Kirby diagrams:*

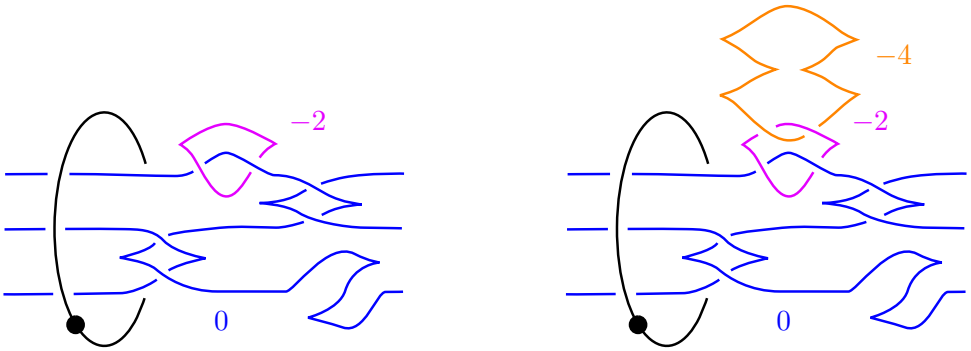

Figure 4.23: Kirby diagrams for $\Sigma_2(B^4, A')$ and $\Sigma_2(B^4, T')$ in standard form.

In particular, they admit Stein structures.

Proof. We present the computation for $\Sigma_2(B^4, A')$, as the other is the same by adding and tracking an extra 2-handle throughout this proof. As always, we start with a Kirby diagram of the complement $B^4 \smallsetminus \nu A'$:

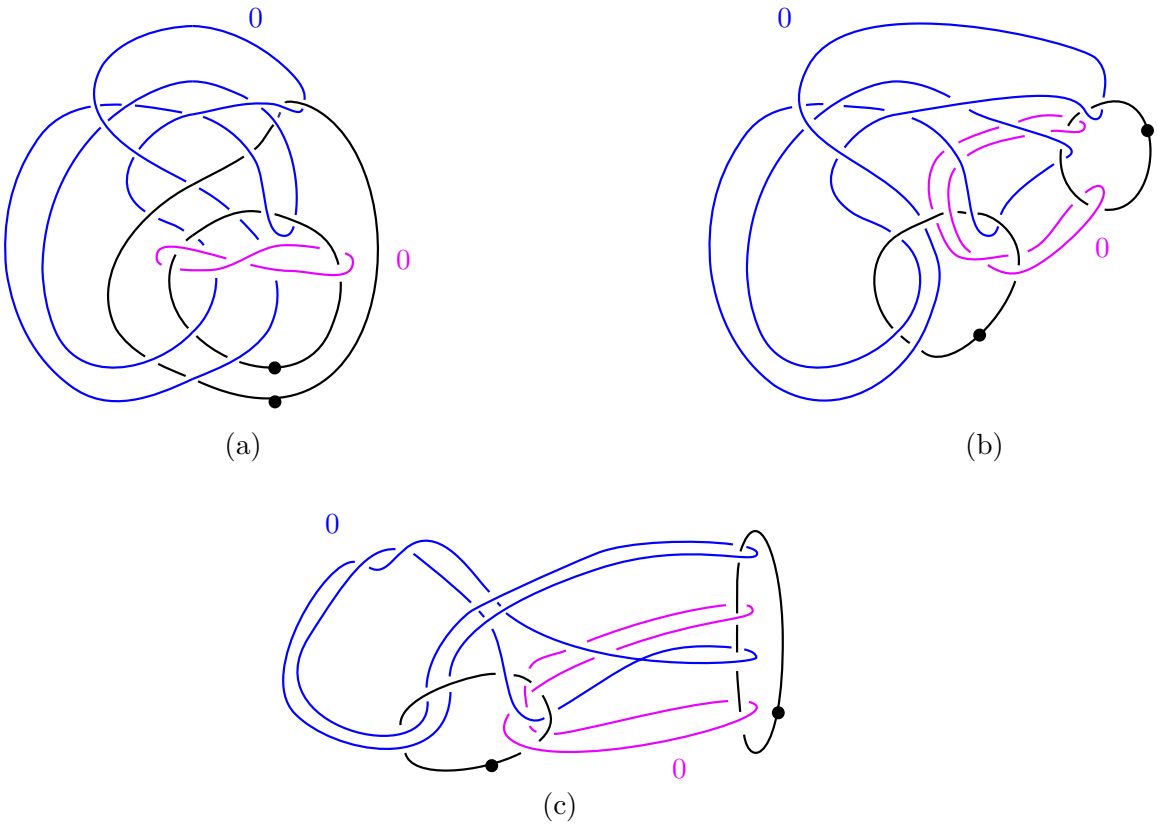

Figure 4.24: Kirby diagrams of $B^4 \smallsetminus \nu A'$.

We then apply Lemma 1.3.8 and lift cancelling handles to obtain Figure 4.25 below. Now, notice that this is exactly the same diagram as the one we had in Figure 4.11 when proving Lemma A.1, except for the purple extra -2-framed 2-handle. Hence, in order to simplify this diagram we follow the same steps as we did above while tracking this extra purple 2-handle. We obtain the leftmost Kirby diagram of Figure 4.23.

Finally, both double branched covers $\Sigma_2(B^4, A')$ and $\Sigma_2(B^4, T')$ admit Stein structures, as every framing coefficient equals $tb - 1$, as required by Theorem 2.2.4.

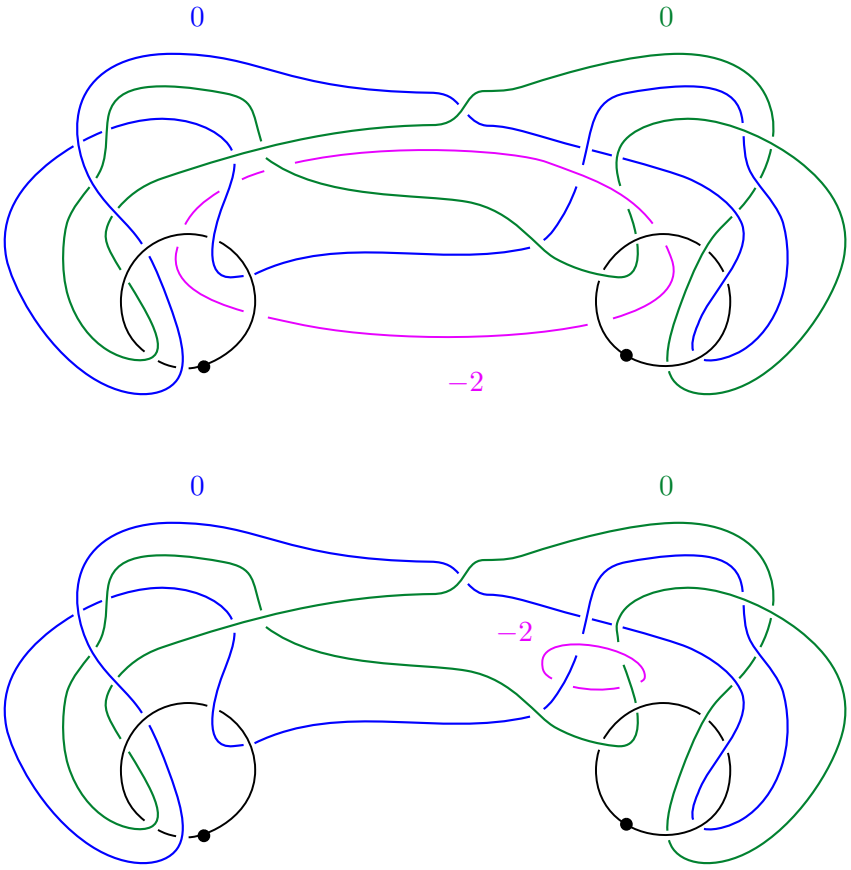

Figure 4.25: Kirby diagrams of $\Sigma_2(B^4, A')$.

□

Lemma A.4. *The double branched cover $\Sigma_2(B^4, M)$ has Kirby diagram:*

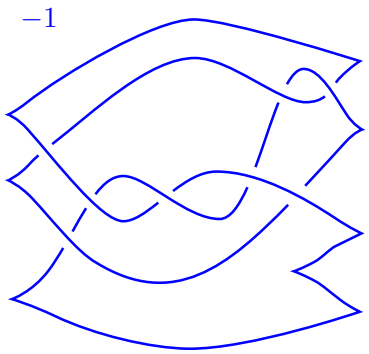

Figure 4.26: Kirby diagram for $\Sigma_2(B^4, M)$.

The shown attaching sphere has $tb = 0$ and hence $\Sigma_2(B^4, M)$ admits a Stein structure.

Proof. We start by producing a Kirby diagram of the complement $B^4 \setminus \nu M$ and making it look like in Lemma 1.3.8. This is done in Figure 4.27.

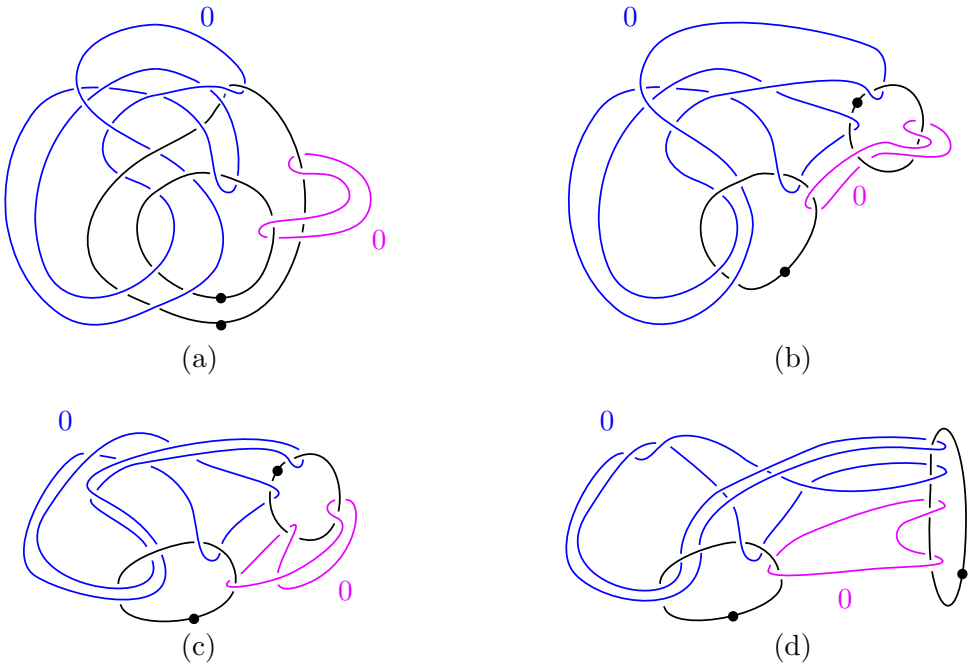

Figure 4.27: Equivalent Kirby diagrams of $B^4 \setminus \nu M$. From (a) to (b), we have performed a 1-handle slide. The other steps are simply isotopies.

Now we can use Lemma 1.3.8 to produce a Kirby diagram of the double cover of $B^4 \setminus \nu M$. Notice that in order to recover B^4 from $B^4 \setminus \nu M$, we need to attach a 2-handle to cancel the rightmost dotted circle and a 3-handle to cancel the blue 2-handle. Hence, we obtain the following Kirby diagram diagram of $\Sigma_2(B^4, M)$ after cancelling the 1-/2-handle pair:

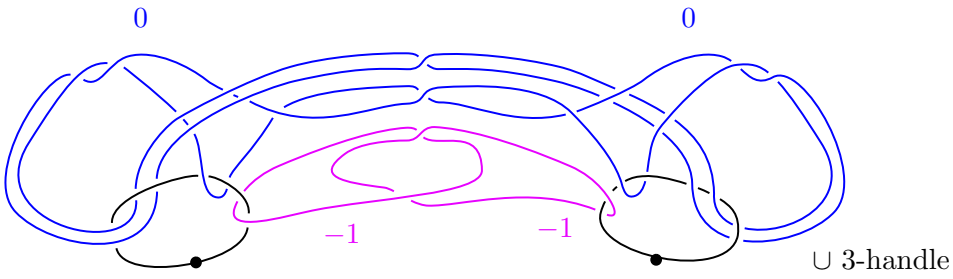

Figure 4.28: Kirby diagram of $\Sigma_2(B^4, M)$ before cancelling the 2-/3-handle pair.

The following steps are simplifications of the diagram above:

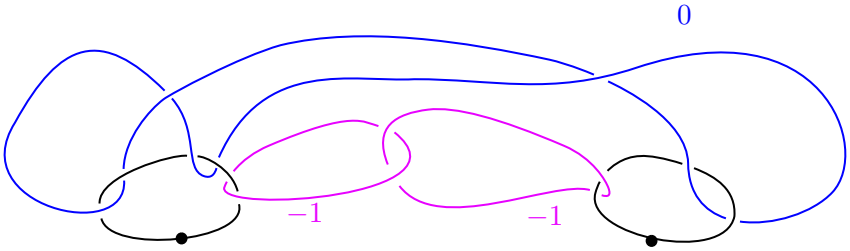

Figure 4.29: Kirby diagram of $\Sigma_2(B^4, M)$ after cancelling the 2-/3-handle pair.

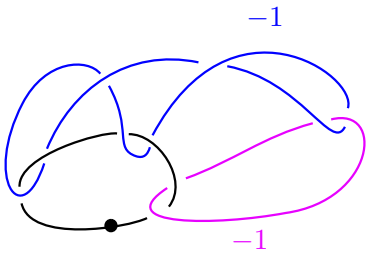

Figure 4.30: Kirby diagrams of $\Sigma_2(B^4, M)$ after sliding the blue 2-handle over the rightmost pink one and cancelling the 1-/2-handle pair.

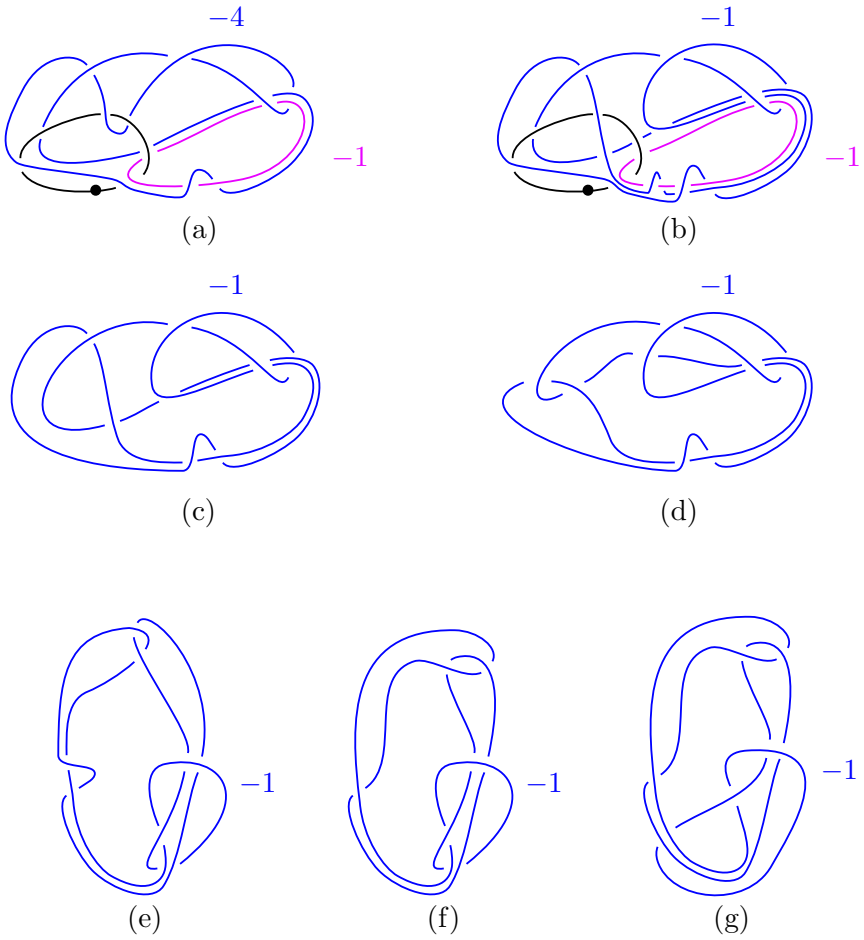

Figure 4.31: Equivalent Kirby diagrams of $\Sigma_2(B^4, M)$. At (a), we have slid the blue 2-handle over the pink one. At (b), we have again done that so that the blue 2-handle does not go through the 1-handle anymore. At (c), we have cancelled the 1-/2-handle pair. The other steps are simply isotopies.

Notice that the diagram (g) is isotopic to the diagram of Figure 4.26. □

Bibliography

[1] S. Abhyankar and T.-t. Moh, *Embeddings of the line in the plane.*, Journal für die reine und angewandte Mathematik, 276 (1975), pp. 148–166.

[2] S. Behrens, B. Kalmar, M. H. Kim, M. Powell, and A. Ray, *The Disc Embedding Theorem*, Oxford University Press, 07 2021.

[3] A. Conway and M. Powell, *Characterisation of homotopy ribbon discs*, Advances in Mathematics, 391 (2021), p. 107960.

[4] C. L. Curtis, Freedman, H. M. H., W. C., and R. Stong, *A decomposition theorem for h-cobordant smooth simply-connected compact 4-manifolds*, Inventiones mathematicae, 123 (1996), pp. 1432–1297.

[5] G. Darboux, *Sur le problème de pfaff*, Bull. Sci. Math., 6 (1882), pp. 49–68.

[6] R. D. Edwards and R. C. Kirby, *Deformations of spaces of imbeddings*, Annals of Mathematics, 93 (1971), pp. 63–88.

[7] Y. Eliashberg, *Topological characterization of stein manifolds of dimension ¿ 2*, International Journal of Mathematics, 01 (1990), pp. 29–46.

[8] J. B. Etnyre, *Legendrian and transversal knots*, (2003).

[9] S. M. Finashin, M. Kreck, and O. Y. Viro, *Exotic knottings of surfaces in the 4-sphere*, Bulletin (New Series) of the American Mathematical Society, 17 (1987), pp. 287 – 290.

[10] R. Fintushel and R. J. Stern, *Symplectic surfaces in a fixed homology class*, Journal of Differential Geometry, 52 (1999), pp. 203 – 222.

[11] J. Globevnik, *On fatou-bieberbach domains*, Mathematische Zeitsschrift, 229 (1998), pp. 91 – 116.

[12] R. E. Gompf, *Handlebody construction of stein surfaces*, 1998.

[13] ——, *Topologically trivial proper 2-knots*, 2023.

[14] R. E. Gompf and A. Stipsicz, *4-Manifolds and Kirby Calculus*, American Mathematical Society, 1999.

[15] V. Guillemin and A. Pollack, *Differential Topology*, AMS Chelsea Publishing, AMS Chelsea Pub., 2010.

[16] A. Hatcher, *Algebraic Topology*, Cambridge University Press, 2001.

[17] K. Hayden, *Corks, covers and complex curves*, (2021).

[18] ——, *Exotically knotted disks and complex curves*, 2021.

[19] K. Hayden and I. Sundberg, *Khovanov homology and exotic surfaces in the 4-ball*, Journal für die reine und angewandte Mathematik (Crelles Journal), 2024 (2024), pp. 217–246.

[20] P. Lisca and G. Matić, *Stein 4-manifolds with boundary and contact structures*, Topology and its Applications, 88 (1998), pp. 55–66. Symplectic, Contract and Low-Dimensional Topology.

[21] J. Milnor, L. Siebemann, and J. Sondow, *Lectures on the H-Cobordism Theorem*, Princeton University Press, 1965.

[22] J. Milnor, M. Spivak, and R. Wells, *Morse Theory. (AM-51), Volume 51*, Princeton University Press, 1969.

[23] L. Rudolph, *Algebraic functions and closed braids*, Topology, 22 (1983), pp. 191–202.

[24] L. Rudolph, *Braided surfaces and seifert ribbons for closed braids*, Comentarii Mathematici Helvetici, 58 (1983), pp. 1–37.

[25] J.-L. Stehle, *Plongements du disque dans c2*, in Séminaire Pierre Lelong (Analyse) Année 1970–1971, Berlin, Heidelberg, 1972, Springer Berlin Heidelberg, pp. 119–130.